ARK5 Regulates Subcellular Localization of hnRNP A1 During Hypertonic Stress

By Travis Richard

A thesis submitted to the Faculty of Graduate and Postdoctoral Studies (FGPS), University of Ottawa, in partial fulfillment of the requirements for the degree of
Master of Science in Biochemistry

Department of Biochemistry, Microbiology, and Immunology
Faculty of Medicine
University of Ottawa

Abstract

During cellular stress, the regulation of protein synthesis is a key adaptive mechanism used by cells to survive. In response to various stresses, heterogeneous nuclear ribonucleoprotein A1 (hnRNP A1), an RNA binding protein principally found within the nucleus, is phosphorylated and consequently accumulates in the cytoplasm. Among other roles, cytoplasmic hnRNP A1 functions as an auxiliary translation factor for internal ribosome entry site (IRES)-mediated translation of specific mRNA, including the anti-apoptotic protein B-cell lymphoma-extra large (Bcl-xL). To identify which kinases control the cytoplasmic accumulation of hnRNP A1, an RNAi-based kinome-wide screen was performed in hypertonically stressed U2OS cells, from which AMPK-related kinase 5 (ARK5) was identified as a potential regulator of hnRNP A1's localization. Here we show that ARK5 directly phosphorylates hnRNP A1 and that the inhibition of ARK5 expression blocks the stress induced cytoplasmic accumulation of hnRNP A1, modulates expression of Bcl-xL protein and increases cell viability. Our data points to a novel role for ARK5 and provides further insight into the mechanisms regulating cellular stress response.

Acknowledgements

I would like to take this opportunity to express my sincerest gratitude towards Dr. Martin Holcik for his expert advice, help, guidance, and enthusiasm that he has provided me with throughout my time working in his lab as his student. I am truly thankful for having been given this opportunity. I would like to express my thanks toward my thesis advisory committee members, Dr. Tommy Alain and Dr. David Stojdl, for taking the time to help me with becoming a better student, researcher and writer through their helpful insight and discussion towards improving my research. I would also like to thank all current and previous members of the Dr. Holcik lab and the Apoptosis Research Center for your friendship, advice and the general day to day, making it so easy to come to the lab. Finally, I would like to express my gratitude to my family, because I would not be the person I am today, nor would I have accomplished what I have without their constant support, love and encouragement.

Table of Contents

List of Abbreviations

a.a.	Amino acid
AMPK	Adenosine monophosphate-activated protein kinase
Apaf-1	Apoptotic protease activating factor 1
ARK5	AMPK-related kinase 5
ATP	Adenosine triphosphate
Bax	Bcl-2-like protein 4
Bcl-2	B-cell lymphoma 2
Bcl-xL	B-cell lymphoma-extra large
BRSK1	BR serine/threonine-protein kinase 1
BSA	Bovine serum albumin
Co-IP	Co-immunoprecipitation
CTRL	Control
DMEM	Dulbecco's modified eagle's medium
DMSO	Dimethyl sulfoxide
DNA	Deoxyribonucleic acid
DTT	Dithiothreitol
ECL	Enhanced chemiluminescence
EDTA	Ethylenediaminetetraacetic acid
eIF	Eukaryotic initiation factor
ERK8	Extracellular signal-regulated kinase 8
EV	Empty vector
FBP1/2	Fructose-1,6-bisphosphatase

FBS	Foetal bovine serum
Frag.	Fragment
GCN2	General control non-derepressible-2
GST	Glutathione S-transferase
GTP	Guanosine-5'-triphosphate
HK2	Hexokinase 2
hnRNP A1	Heterogeneous nuclear ribonucleoprotein A1
HRI	Haem-regulated inhibitor kinase
HRV	Human rhinovirus
IHPK3	Inositol hexakisphosphate kinase 3
IRES	Internal ribosome entry site
ITAF	IRES *trans*-acting factor
LB	Luria broth
MAPK11	Mitogen-activated protein kinase 11
mRNA	Messenger RNA
mRNP	Messenger ribonucleoprotein complex
Mut.	Mutant
NES	Nuclear export signal
NLS	Nuclear localization signal
NUAK1	NUAK family SNF1-like kinase 1
OXSR1	Serine/threonine-protein kinase OSR1
P/S	Penicillin / Streptomycin
PAGE	Polyacrylamide gel electrophoresis

PBS	Phosphate-buffered saline
PDCD4	Programmed cell death 4
PERK	PKR-like endoplasmic reticulum kinase
PKR	Protein kinase RNA
PMSF	Phenylmethylsulfonyl fluoride
PP1β	Protein phosphatase 1 beta
PSKH2	Protein serine kinase H2
PTB	Phosphotyrosine-binding
PVDF	Polyvinylidene difluoride
RBD	Ribosomal binding domain
RIPA	Radioimmunoprecipitation assay
RNA	Ribonucleic acid
RPM	Revolutions per minute
RRM	RNA recognition motif
SDS	Sodium dodecyl sulfate
siRNA	Small interfering RNA
TBS	Tris-buffered saline
U2OS	Human bone osteosarcoma epithelial cells
uORF	Upstream open reading frame
UTR	Untranslated region
UV	Ultraviolet
WT	Wild type
XIAP	X-linked inhibitor of apoptosis protein

List of Figures and Tables

Chapter 1: Introduction

1.1 Stress Response

Survival is an innate skill intrinsic to all living things which instils the constant flow between two opposing states of being, homeostasis and disequilibrium. The ability to adapt and survive is based on a multitude of aspects, including resources and capabilities. These adaptations range from micro to macro, inciting post-translational modifications and cascading effects leading to the activation of multiple signaling pathways. As such, cells require the ability to identify signals and changes in their microenvironment, as well as being capable of alterations in both their physical and biochemical aspects to adapt (Katz *et al*, 2016).

Adaptation is an ever-present form of compensation used by cells to become accustomed to an adverse environment. Stress inducing conditions such as, but are not limited to, osmotic shock, nutrient deprivation and heat shock can cause disequilibrium within a cell and its surroundings (Guil *et al*, 2006; Komar and Hatzoglou, 2011; Liwak *et al*, 2012a). For example, excessive heat applied to the cell leads to a protective heat shock response and therefore the expression of chaperone proteins to promote protein folding, resulting in thermobalance (Fulda *et al*, 2010; Samali *et al*, 1999). The presence of oxidative stress leads to an imbalance of pro-oxidants and anti-oxidants causing redox cycling to take place to re-establish a balance (Fulda *et al*, 2010). Hyperosmolarity in the cellular milieu leads to cell shrinkage, DNA damage and cell cycle arrest (Brocker *et al,* 2012). To compensate for these changes a cell can undergo both physical and chemical changes, such as cytoskeletal rearrangement and osmolyte synthesis (Burg *et al*, 2007). In short, when in the presence of a stress, our cells can change both biochemically and structurally to restore homeostasis and maintain their proper function. To accomplish this, multiple signaling

pathways are altered as to ensure a cell's survival (Holcik and Sonenberg, 2005). In all cases, the mechanisms a cell uses to deal with stress are dependent on the type, the severity and the duration of the stress.

All in all, so long as the noxious stimuli does not first overwhelm the cell by means of intensity or duration, there are a plethora of mechanisms a cell can use to endure environmental stressors (Fulda *et al*, 2010). However, if the insult does persist well past the threshold of tolerance the cell will undergo some form of cell death program, be it apoptosis, necrosis, or autophagic cell death, depending often on how well the cell copes with the incident and the presented conditions (Fulda *et al*, 2010).

One of the main underlying mechanism that cells use to maintain and achieve homeostasis is through the regulation of protein synthesis, either by cap-dependent or independent translation (Holcik and Sonenberg, 2005).

1.2 Cap-dependent Translation

Under normal physiological conditions, proteins are proportionately synthesized based on their need for proper function and stoichiometric balance (Li *et al,* 2014). As it is well described in the literature, the production of specific or essential proteins is highly regulated and is crucial for the well-being of the cell (Liwak *et al,* 2012a). As such, complex molecular machinery is required to synthesize the required resources. For this machinery, there are two predominant mechanisms that are commonly used, the cap-dependent mechanism and the cap-independent mechanism from

which the former produces the majority of proteins found in the cell, 95-97%, and the latter is responsible for 3-5 % (Komar and Hatzoglou, 2015).

Between the two mentioned, literature states that the cap-dependent mechanism is accountable for the majority of protein translation under steady state conditions and requires multiple steps to initiate the recruitment of translation factors and complexes to be accomplished (Holcik and Sonenberg, 2005). As stated above, one of the main methods of survival for a cell is the regulation of protein synthesis, which is because the synthesis of proteins is exceedingly demanding in terms of cellular energy compared to many other cellular processes (Liwak *et al,* 2012a). In addition, translation initiation is often considered the rate limiting step of protein synthesis more so than elongation or termination (Holcik and Sonenberg, 2005). Within this mechanism, the cap-dependent translation begins the initiation through the activation and migration of mature mRNA in the form of mRNP complexes from the nucleus to the cytoplasm (Glisovic *et al,* 2008). Once the mRNA is activated, the secondary structures and associated proteins are removed in an ATP-dependent manner to ensure that, in the cytoplasm, the initiation complex can bind (Richard *et al,* 2010). While in the cytoplasm, the eIF4F complex, made up of cap-binding protein eIF4E, ATP-dependent RNA helicase eIF4A, and scaffolding protein eIF4G, recognizes the 5'm^7G cap of mRNA's UTR (Komar and Hatzoglou, 2015; Liwak *et al,* 2012a). In concomitance, the formation of the 43S pre-initiation complex is formed through the recruitment of 40S ribosomal subunit, eIF3, eIF1/1A, in which the initiator ternary complex eIF2(α,β, and γ)-GTP-methionyl transfer RNA binds to the P site in the 40S subunit (Holcik, 2015; Liwak *et al,* 2012a; Richard *et al,* 2010). Once the two are formed, eIF4G and eIF3 communicate with one another to pull the two complexes together ultimately forming the 43S ribosome, which subsequently begins to scan the mRNA

sequence for the start codon, often found as AUG (Holcik and Sonenberg, 2005; Liwak *et al,* 2012a). Once found, the 48S pre-initiation complex is formed and the recruitment of the 60S ribosome is completed by means of an irreversible hydrolysis of eIF2 bound GTP by eIF5, allowing the creation of the 80S complex (Komar and Hatzoglou, 2015; Richard *et al,* 2010). This instigates the release of eIFs from the complex to be recycled and elongation ensues (Liwak *et al,* 2012a).

1.3 Cap-independent and Selective Translation

An important fact is that when the insult of stress is brought onto cells, be it by means of physiological or pathological reasons, the aforementioned cap-dependent translation mechanism is hindered (Liwak *et al,* 2012a). One aspect of this result is thought to be brought on by the phosphorylation of a stress regulator, eIF2α, which occurs during periods of extreme stress at residue Ser51 by one of the four stress induced kinases, Haem-regulated inhibitor kinase (HRI), protein kinase RNA (PKR), PKR-like endoplasmic reticulum kinase (PERK), and general control non-derepressible-2 (GCN2) (Holcik and Sonenberg, 2005). In the case of severe hypertonic shock, once eIF2α is phosphorylated, formation of the ternary complex, eIF2-GTP-$tRNA_iMet$, is inhibited, which cascades into the loss of normal cellular mRNA translation initiation (Bevilacqua *et al*, 2010). This also results in the concomitant loss of osmoadaptation, increased stress granule formation, the attenuation of anti-apoptotic programs and encourages the translation initiation of select proteins responsible for stress response (Bevilacqua *et al*, 2010). In addition, eIF2α phosphorylation is shown to influence the cytoplasmic accumulation of hnRNP A1, along with hnRNP A1 being sequestered into stress granules accompanied by repressed mRNA (Bevilacqua *et al*, 2010). However, the precise mechanism of eIF2α-hnRNP A1 link is not known. In real time,

when stress is present and has not overwhelmed the cell, the ability to synthesize select proteins to instigate a reversal of unfavorable conditions found surrounding the cell is essential. These select proteins are often meant to boaster a cell's defense and, if circumstances allow, the reversal of damage, leading to its eventual recovery. As such, alternative methods are necessary to produce the required proteins. One method of selective translation uses upstream open reading frames (uORFs), a stretch of codons containing both the initiation and termination codons found within the 5' UTR, upstream of the AUG found in the primary open reading frame (Barbosa *et al,* 2013). While in the presence of stress, as for example, under conditions that would incite the phosphorylation of eIF2α and attenuate global protein synthesis, uORFs have been noted to be used as the means to regulate the translation of specific stress related mRNAs (Barbosa *et al,* 2013). Another example of an alternative method of protein synthesis is a mechanism known as internal ribosome entry site (IRES)-mediated translation.

1.3.1 Internal Ribosome Entry Site

Originally observed in picornaviruses, such as poliovirus, and encephalomyocarditis virus, an IRES based translational mechanism was used to describe the ability of viruses to hijack the use of a host's ribosomes all the while hindering the typical proteomic profile and synthesis found within the cell (Holcik, 2015; Komar and Hatzoglou, 2015; Lloyd, 2015). An example of this is when viruses, such as the poliovirus, use viral proteases to cleave eIF4G and therefore hinder host protein production (Gradi *et al,* 1998). As such, these viruses could stop the production of a clear majority of the host's proteins to increase the possibility of their viral proteins to be preferentially expressed, as well as create an increased availability of cellular energy stores for their rapid viral replication (Komar and Hatzoglou, 2015). Through studies there have been the identification of

five distinct viral IRES types, with each using a different mechanism that employs a specific combination of the use of canonical and non-canonical eukaryotic initiation factors, as well as 40S ribosomal subunits (Richard *et al,* 2010; Sweeney *et al,* 2012). Type I, found to be used by the poliovirus and other viruses belonging to the *Enterovirus* genus, is approximately 450 nucleotides in length, is characterized by five domains (II to VI), and initiates translation without the use of eIF4E using eIF4G and eIF4A to recruit the 43S ribosome complex (Richard *et al,* 2010; Sweeney *et al,* 2012). Type II is of a similar length to type I, but is found in viruses such as the encephalomyocarditis virus and others belonging to the *Aphthovirus, Cardiovirus and Parechovirus* genera (Sweeney *et al,* 2012). Type II is also characterized for having five domains (H, I, J, K and L) which vary from those found in type I, yet type II recruits the 43S ribosome complex using eIF4G and eIF4A, without implicating eIF4E, similarly to type I. Type II also uses a different set of non-canonical eIFs than those used by type I IRESs (Sweeney *et al,* 2012). Type III is found to be used by the hepatitis C virus and is smaller in comparison to types I and II at approximately 300 nucleotides in length (Richard *et al,* 2010). This classification of IRES is characterized by its direct interaction with eIF3 and the 40S ribosomal subunit of the 43S complex for its recruitment to the initiation codon, which promotes the subsequent formation of the 48S initiation complex without the use of eIF1, eIF1A, eIF4B, eIF4B and eIF4F (Richard *et al,* 2010; Sweeney *et al,* 2012). Type IV, found to be used by the cricket paralysis virus and is smaller than the other types at approximately 200 nucleotides, recruits and binds directly to the P-site of the 40S ribosome subunit without the use of eIFs or $tRNA_i^{Met}$ (Richard *et al,* 2010). Type V, found to be used by viruses such as Aichi virus and bovine kobuvirus along with other members of the *Kobuvirus, Salivirus,* and *Paraturvirus* genera of the *Picornaviridae* family, is approximately 410 nucleotides in length and requires the DExH-box protein, DHX29 helicase, for the recruitment of

ribosomes (Sweeney *et al,* 2012). In addition, some of these IRESs employ the use of ITAFs, cellular RNA binding proteins used to aid or inhibit the recruitment of ribosomes, to maintain optimal three-dimensional conformation of the IRES domain, as the RNA structure tends to hold great importance for viral IRES functions (Baird *et al,* 2006; Richard *et al,* 2010). It was not too long after the discovery of viral IRESs that the existence of cellular IRESs were contemplated due to viral IRESs using cellular initiation factors and cellular ITAFs to produce proteins.

Despite having been empirically identified in a few mRNA, IRES mediated translation is said to be responsible for 3-5% of mRNA cap-independent translation under stress conditions (Holcik and Sonenberg, 2005; Johannes *et al,* 1999). However, very little has been concretely identified about their mechanism or indefinable characteristics (Holcik and Sonenberg, 2005). In comparison to viral IRESs, which tend to show structural similarities, cellular IRESs are known to have no common sequences or structural motifs which allow for their identification. Typically, IRES regions have been discussed to be found within longer UTRs, they tend to have a greater presence of AUG codons and they tend to have higher levels of complex secondary and tertiary structures such as stem-loops and pseudoknots (Baird *et al,* 2006; Komar and Hatzoglou, 2005). However, these characteristics are not preserved in all cellular IRESs, as, unlike viral IRESs, cellular IRESs show greater diversity in their structure. In terms of mechanism of action, an IRES acts as the site of interaction with canonical and non-canonical translation factors, such as ITAFs, to properly position the ribosomes near the start codon to initiate translation when the use of the cap structure, eIF4E or the ternary complex are no longer viable (Komar and Hatzoglou, 2011). Alongside this, with the theme of stress and disadvantageous conditions for cells, such as pathological states, IRESs have been known to be found in mRNA linked to processes like proliferation, cell survival,

and apoptosis control (Holcik and Sonenberg, 2005). For example, mRNA sequences known to contain an IRES are Bcl-xL, XIAP, c-Myc, p53, and Apaf-1, and even though these mRNAs are capped, the IRES acts, in some cases, as a failsafe to promote recovery following the cellular arrest brought on by stress (Bevilacqua *et al*, 2010; Coldwell *et al,* 2000; Holcik *et al,* 1999; Ray *et al,* 2006; Stonely *et al*, 1998). Alternatively, this could be why it is believed that through evolution, IRESs tend to show greater resistance to stress induced decline in protein synthesis (Holcik *et al,* 2000).

1.3.2 IRES *Trans*-acting Factor

To be fully realized, IRES-mediated translation involves not only canonical eukaryotic translation initiation factors, they often require the additional presence of auxiliary proteins known as an IRES *trans*-acting factor (ITAF) (Spriggs *et al,* 2005). Unfortunately, the exact mechanism to which an ITAF can enable the IRES-mediated recruitment of ribosomes to initiate translation is not fully understood (Lewis and Holcik, 2007). Most ITAFs to date have been identified as RNA binding proteins, which serve other roles in the cell such as mRNA splicing, export, stress granule formation and translation initiation (Liwak *et al,* 2012a). To name a few examples, some previously identified ITAFs are hnRNP A1, hnRNP C1/C2, HuR, and PDCD4, (Durie *et al,* 2011; Holcik *et al,* 2003; Jo *et al*, 2008; Liwak *et al.*, 2012b). Interestingly, ITAFs have been noted to act both as positive and negative regulators for IRES-mediated translation. One mechanism that has been proposed for the regulation of IRES-mediated translation is that an ITAF, with or without canonical translation factors, is used to either create or destroy bonds between the mRNA and ribosome to facilitate or hinder translation initiation (Komar and Hatzoglou, 2005). Another proposed mechanism is an ITAF can alter an IRES's complex secondary and tertiary structure,

resulting in the change to its conformation either to favor or impede translation (Komar and Hatzoglou, 2005). Additionally, ITAFs have been noted to be regulated based on either their subcellular localization or their concentration within a cell (Lewis and Holcik, 2007; Spriggs *et al,* 2005). In regards to this study, the ITAF of interest is hnRNP A1, an RNA binding, nucleocytoplasmic shuttling protein.

1.4 RNA Binding Proteins

RNA binding proteins play an important role in the regulation of gene expression, from tasks that include, but are not limited to, splicing, nuclear export, stability and the translation of mRNA (Jean-Philippe *et al,* 2013). Amongst this category of proteins, is the prevalent and most studied family, hnRNPs. This family consist of 20 members, referred to as hnRNP A through to hnRNP U, ranging in sizes of 34 to 120 kDa (Piñol-Roma *et al,* 1988). The important characteristics of this class are identified by their globular domains, RNA recognition motifs, and RGG boxes (Jean-Philippe *et al,* 2013). Within this group, the most abundant and best studied is hnRNP A1 and, as noted above, hnRNP A1 is a confirmed ITAF as well as a focus point in this project.

1.4.1 Heterogeneous Nuclear Ribonucleoprotein A1

Asides from being an RNA binding protein, hnRNP A1 is also characterized as a nucleocytoplasmic shuttling protein. Physical traits wise, hnRNP A1 is most noted for two, in tandem, RRMs found in the N-terminal region, each responsible for the specificity in binding of RNA, followed by a glycine-rich domain housing the RBD RGG box, responsible for the homologous and heterologous interactions with other RBPs and RNA, and, finally, two regions referred to as the M9 sequence, a 38 amino acid region which acts as the protein's NLS and NES,

and the F-peptide, playing a role in transportin-dependent import (Allemand *et al*, 2005; Jean-Philippe *et al,* 2013). Typically, hnRNP A1 is found within the nucleus at a physiological steady state, however, hnRNP A1 is in a constant state of flux, as hnRNP A1 is continuously shuttling between the nucleus and the cytoplasm. It is believed that the reason why it is found predominantly in the nucleus during an analysis by immunofluorescence is that the turnover rate to which hnRNP A1 stays in the cytoplasm is incredibly short (Izaurralde *et al,* 1997; Siomi and Dreyfuss, 1995). However, it is believed that this localization mechanism can be altered depending on the post-translational modifications (Jean-Philippe *et al,* 2013). Within hnRNP A1, studied sites of post-translational modification include, but are not limited to, the M9 sequence and F-peptide, which both influence the localization mechanism of hnRNP A1. With the onset of stresses such as UV irradiation and hypertonic shock, one of the chain events includes the phosphorylation of hnRNP A1 in the F-peptide regions (Iijima *et al,* 2006; Van der Houven van Oordt *et al,* 2000). It has been proposed that the phosphorylation of the juxtaposed F-peptide to the M9 sequence causes a conformational change in the C-terminal end of hnRNP A1 leading to the lack of interaction between the M9 sequence and the β-karyopherins, transportin 1 and 2, which are believed to be a source of migration for hnRNP A1 through nuclear pore complexes (Allemand *et al*, 2005; Nakielny *et al,* 1996; Rebane *et al,* 2004; Twyffles *et al,* 2014). With the loss of this interaction, comes the loss of nuclear import and therefore a resulting accumulation of hnRNP A1 within the cytoplasm (Allemand *et al*, 2005).

As an ITAF, hnRNP A1 serves to promote or inhibit the selective translation of mRNAs containing IRES elements such as XIAP, Apaf-1, c-Myc, FGF-2, cyclin-D1, SREBP-1a and Bcl-xL (Bevilacqua *et al*, 2010; Bonnal *et al,* 2005; Cammas *et al,* 2007; Damiano *et al,* 2013; Jo *et al*,

2008; Lewis *et al,* 2007). For this project, the target of interest is Bcl-xL due to its interaction with shock induced cytoplasmic hnRNP A1 which is shown to suppress Bcl-xL's IRES-mediated translation (Bevilacqua *et al*, 2010). Bcl-xL is an anti-apoptotic protein belonging to the Bcl-2 family (Um, 2015). This family is composed of multiple proteins known as key regulators of either apoptosis suppression or promotion (Um, 2015). For example, pro-apoptotic members of this family are capable of inducing permeabilization of the outer membrane of the mitochondria, releasing cytochrome C and activating cascading effects toward the death of the cell (Chipuk *et al, 2006*). However, the pro-survival members, typically interact with the promoters of cellular death to inhibit their activation. Bcl-xL, is an anti-apoptotic member that is capable of hindering apoptosis using one of three methods: i) Bcl-xL binds with Apaf-1, a key player in mitochondrial apoptosis pathway, to prevent its activation which subsequently leads to the activation of caspase-9 (Hu *et al,* 1998); ii) Bcl-xL inactivates caspase-8 (Wang *et al,* 2004); and iii) Bcl-xL interacts with Bax, a pro-apoptosis member of Bcl-2, to inhibit its activation (Ma *et al,* 2016). Along the lines of apoptosis, it is due in part to this link that hnRNP A1 is often studied in terms of pathology, as hnRNP A1 is often deregulated in many cancers and neurodegenerative diseases (Levin *et al,* 2016; Perrotti and Neviani, 2007). Analysis and a full understanding of the workings of hnRNP A1 proves to be an interesting topic for pharmacological studies.

Overall, the main purpose of this study is to identify and explore the mechanism behind the phosphorylation of hnRNP A1. To do this, a study was performed by reverse transfection on U2OS cells with an arrayed library of microRNAs to target 691 genes related to the human kinome in hopes of identifying kinases that regulate hnRNP A1's localization during hypertonic stress conditions (Courteau *et al,* 2015) (Figure 3.1). From this analysis, a list of potential kinases were

identified including HEK2, ARK5, ERK8, MAPK11, OXSR1, PSKH2, IHPK3, and BRSK1 (Courteau *et al,* 2015). Of which, the kinase of interest for this study is ARK5.

1.5 AMPK-related Kinase 5

Adenosine monophosphate-activated protein kinase (AMPK) is a well-known critical regulator of whole body and cellular energy metabolism (Sun *et al,* 2013). However, unfortunately, not much has been fully characterized of the other 12 AMPK-related kinases belonging to the same family, which share some significant structural similarities (Sun *et al,* 2013). Of these related proteins, AMPK-related kinase 5 (ARK5) has structural characteristics which include a N-terminal catalytic domain, an ubiquitin-associated domain, and a C-terminal housed kinase-associated domain (Sun *et al,* 2013). ARK5 is acknowledged for being highly expressed or deregulated in colon, pancreas, breast and glioma cancers, to name a few, and both mRNA and protein is found in heart, kidney, brain, liver and skeletal muscle tissues (Chang *et al,* 2012; Lu *et al,* 2013; Sun *et al,* 2013). In addition, ARK5 is not only deregulated or over-expressed in many pathologies, but plays an important role in cell survival, tumor progression, invasion and metastasis (Banerjee *et al,* 2014b; Chang *et al,* 2012). Some of these roles have been noted to be caused by stressors, such as nutrient deprivation, which induces the activation of ARK5 through phosphorylation by Akt at Ser560 and LKB1 at Thr211 leading to ARK5 interacting with targets such as the synthetic SAMS peptide, $PP1\beta^{MYPT1}$, p53, and caspase 6 (Banerjee *et al,* 2014b; Hou *et al,* 2011; Suzuki *et al,* 2003).

1.6 Rationale, Hypothesis and Objectives

Previous research has identified that the regulation of protein synthesis is critical in the response to stress which can lead to altered viability for the cell. As such, part of the response to hypertonic

stress is the relocalization of hnRNP A1 and its concomitant accumulation in the cytoplasm thought to be caused by phosphorylation (Van der Houven van Oordt *et al,* 2000). However, despite that this mechanism has yet to be fully understood, it is proposed that while hnRNP A1 is accumulated in the cytoplasm, it can interact with targets such as Bcl-xL and is sequestered into stress granules (Bevilacqua *et al*, 2010; Guil *et al*, 2006). In addition to this, hnRNP A1 is used as an ITAF in cells to aid in the regulation of IRES-mediated selective translation to respond to hypertonic stress. I therefore hypothesize that ARK5 regulates hnRNP A1's response to stress and by extension its subcellular localization by phosphorylation. To test this hypothesis, I first set out to validate the results of the RNAi-based kinome-wide screen using siRNA mediated knockdown of ARK5, ARK5 overexpression rescue and ARK5 inhibitory drug treatments. Second, I investigated the mechanism by which ARK5 affects hnRNP A1 localization, and finally, I explored the effects of ARK5 mediated localization of hnRNP A1 on cell survival during hypertonic stress.

Chapter 2: Methods and Materials

2.1 Cell Culture and Transfection

U2OS cells were cultured in complete HyClone™ High-Glucose Dulbecco's Modified Eagle's Medium (DMEM) (Thermo Scientific) supplemented with 10% Heat-Inactivated Foetal Bovine Serum, 1% L-Glutamine, $1x10^5$U/L Penicillin, and 100g/L Streptomycin at 37°C with 5% CO_2.

For the siRNA mediated knockdowns, $2x10^5$ U2OS cells were seeded into the wells of a 6 well culture plate and cultured in complete DMEM for a period of 24 hours. Following this, cells were transfected using Lipofectamine® RNAiMAX transfection reagent (Invitrogen) and the manufacturer's protocol with 20nM of either Negative Control siRNA (Quiagen, Cat.# 1027310), ON-TARGETplus Human NUAK1 siRNA (Dharmacon, Cat.# J-004931-12) (referred to in paper as siARK5 and siARK5 #2), or siARK5 #1 (Supplied by Dr. Lewis, ACRI) as per the requirements of the experiment in question and maintained for 24 hours in DMEM without P/S at 37°C with 5% CO_2.

For the overexpression of specific proteins, cells were seeded and cultured in an identical manner as knockdowns during the first 24 hours. Subsequently, cells were transfected with 0.25μg of either a control plasmid (pmKate2-C, referred to as EV) or a plasmid expressing GST-tagged ARK5, or with 1μg of plasmids expressing FLAG-hnRNP A1, FLAG-hnRNP A1 (ΔM9), FLAG-hnRNP A1 (F2), FLAG-hnRNP A1 SASSS mutants, FLAG-tagged fragments of hnRNP A1, or FLAG (referred to as FLAG control) using jetPRIME® transfection reagent (Polyplus) and the manufacturer's protocol. Transfected cells were maintained at 37°C with 5% CO_2 in DMEM without P/S for 4 hours, at which point the media containing the plasmid in question was removed

and fresh DMEM without P/S was added, without rinsing the wells, then subsequently returned to 37°C with 5% CO_2 for the following 20 hours.

For rescue experiments, cells were seeded with $1x10^5$ cells per well onto a 6 well culture plate, then maintained for 24 hours at 37°C with 5% CO_2. The next day, the previously discussed siRNA knockdown method was applied for 24 hours, followed by the subsequent overexpression transfection of desired plasmids for 24 hours using the above directions, after which cells were hypertonically shocked, then collected.

2.2 Hypertonic Shock

For hypertonic shock, cells were rinsed with 2mL of PBS, followed by the subsequent addition of either warmed complete DMEM media (negative control) or 2mL of a 0.5M D-Sorbitol (Sigma-Aldrich) solution in complete DMEM. The stress was performed at 37°C with 5% CO_2 for 2 hours, at which point media was removed and cells rinsed, then collected.

2.3 Cloning and Mutagenesis

To create the expression vectors for the hnRNP A1 fragments (1, 2, 3, 1+2, and 2+3) housed in a pcDNA3 backbone, first, with a pCI plasmid expressing FLAG-hnRNP A1 as the template, a PCR was performed using PfuUltra II Fusion HS DNA Polymerase (Agilent) (primers used are found in the Appendix), followed by a DNA restriction digest using EcoRI and XbaI (Invitrogen) to create the desired sequence for the insert. Afterwards, a ligation was performed using a T4 DNA ligase (Invitrogen) while following the manufacturer's protocol to bind the desired insert and the vector pcDNA3, which was subsequently transformed into DH5α *E. coli*, then plated onto a culture

plate containing LB agar with 100μg/mL of ampicillin. The next day colonies were selected and grown into a 4mL LB broth with 100μg/mL of ampicillin culture overnight. Using a QIAprep® Spin Miniprep Kit (Qiagen), plasmids were isolated, then the presence of the proper insert was confirmed by DNA enzyme digestion. All sequences were confirmed by sequencing (StemCore Laboratories, OHRI).

Mutagenesis for the FLAG-tagged hnRNP A1 SASSS mutants was performed by PCR using PfuUltra II Fusion HS DNA Polymerase (Agilent) (primers used are found in the Appendix). The template used for hnRNP A1 SASSS mutant 1 was a pCI vector expressing FLAG-tagged hnRNP A1, hnRNP A1 SASSS mutant 2 was generated using FLAG-hnRNP A1 SASSS mutant 1. Mutant 1 includes mutations S188A, S190A, and S191A, and mutant 2 includes mutations S188A, S190A, S191A, and S192A. Following the PCR, samples were treated with DpnI (NEB), then transformed into TOP10 competent cells. Cells were then plated onto culture plates with LB agar with 100μg/mL of ampicillin and set to incubate overnight at 37°C. After selecting colonies from these culture plates to be grown, the isolation, confirmation and sequencing of plasmids were performed as described above.

2.4 Protein Purification

GST-tagged proteins: BL21(DE3) *E. coli* expressing the GST-tagged SAMS peptide or GST (both supplied by Dr. Tsuchihara, NCC EPOC) were grown for 24 hours and pelleted by centrifugation at 5000xg for 15 minutes at 4°C. Cell pellets were resuspended in 10mL of cold PBS and centrifuged again, after which the cell pellets were resuspended in 10mL of lysis buffer (50mM Tris-HCl pH8.0, 200mM NaCl, 1mM EDTA, ddH2O supplemented with 1mM DTT and 2mM

PMSF). Lysates were then sonicated on ice at 12% amplification for two sets of 10 seconds with 1 minute break. 100µL of Triton X-100 was added to each lysate, then centrifuged at 4730 RPM for 10 minutes at 4°C and supernatants were collected. 200µL of a 50% slurry of Gluthathione Sepharose™ 4 Fast Flow beads (GE Healthcare) was added, then lysates were set to rotate for 2 hours at 4°C. Once collected, lysates were centrifuged at 500xg for 5 minutes and then rinsed five times with 5mL of PBS. Finally, beads were resuspended in 1mL of PBS and the proteins eluted with the addition of 600µL of L-glutathione pH8.0, while rotating at 4°C for 1 hour. Protein concentration was quantified using Bradford assay.

His-tagged proteins: BL21(DE3) *E. coli* expressing the His-tagged hnRNP A1 and its variants were grown for 24 hours and pelleted by centrifugation at 6000 RPM for 15 minutes at 4°C, then lysed in 20mL of TKGD buffer (20mM Tris-HCl pH7.4, 200mM KCl, and 1% glycerol, supplemented with 1mM DTT, 2 tablets of cOmplete™ Protease Inhibitor Cocktail (Sigma-Aldrich), and 2mg/mL of lysozyme). Samples were kept on ice for 30 minutes prior to adding 5µL DNAse 1 enzyme and 300µL of 1M $MgCl_2$. Samples were sonicated at 25% amplification, six times for an interval of 30 seconds on, 30 seconds off. 0.5mL of Triton X-100 was added to each sample, then set to rotate at 4°C for 30 minutes. Samples were centrifuged at 4730 RPM for 30 minutes at 15°C and supernatant was collected. 0.25 mL of 1M imidazole solution prepared in TKGD buffer was added to each sample, then loaded, one sample at a time, into a HisTrap™ HP column (GE Heathcare) following the manufacturer's protocol. His-tagged proteins were step eluted by increasing concentrations of imidazole solution and each elute was collected, tested via SDS-PAGE, then Coomassie stained to identify the eluate with the highest purity of the protein, which was subsequently dialysed overnight in TKGD buffer at 4°C, then passed through an

Amicon Ultra™ centrifugal filter tube (Millipore) to concentrate. Samples were aliquoted, equal volume 20% glycerol mixed into 2X TKGD buffer was added and stored at -80°C.

FLAG-tagged proteins: U2OS cells were transiently transfected with the desired plasmids expressing FLAG-tagged proteins for 24 hours as described above, cells were rinsed with PBS, then scraped from the wells, recovered in 1mL of PBS and transferred to an Eppendorf 1.5mL tube. Cells were centrifuged at $1.3x10^5$ RPM for 1 minute at room temperature, then supernatant was discarded. Cell pellets were resuspended in 500µL of lysis buffer (50mM Tris-HCl pH7.4, 150mM NaCl, 1mM EDTA, 1% Triton X-100, and supplemented with cOmplete™ Protease Inhibitor Cocktail (Sigma-Aldrich)), then sonicated at 20% amplification for 6 seconds and centrifuged for 20 minutes at $1.3x10^5$ RPM at 4°C. Following the spindown, 50µL of each sample were set aside at -20°C for immunoblotting. 30µL of prepared Anti-FLAG® M2 Affinity Gel (Sigma-Aldrich) beads were added to each sample and then set to rotate for 2 hours at 4°C. Samples were then centrifuged at 6000 RPM for 2 minutes at 4°C, subsequently supernatant was discarded and the beads rinsed in 1mL of TBS. This last step was repeated three times. Beads were then rinsed with 1X kinase buffer (200mM Tris-HCl pH7.5, 50mM β-Glycerolphosphate, ddH_2O, supplemented with 2mM $NaVO_4$ and 2.5µM DTT), then the supernatant was discarded and the affinity gel used in *in-vitro* kinase assays.

2.5 Co-Immunoprecipitation

U2OS cells were transiently transfected with the desired plasmids for 24 hours as described above, the cells were rinsed with PBS, then scraped from the wells, recovered in 1mL of PBS and transferred to an Eppendorf 1.5mL tube. Cells were centrifuged at $1.3x10^5$ RPM for 1 minute at

room temperature, then supernatant was discarded. Cell pellets were resuspended in 500µL of Co-IP buffer (25mM Tris-HCl pH7.4, 150mM NaCl, 50mM NaF, 0.5mM EDTA, 0.5% Triton X-100, 5mM β-glycerophosphate, 5% glycerol, and ddH_2O, supplemented with cOmplete™ Protease Inhibitor Cocktail (Sigma-Aldrich)). Cells were sonicated at 20% amplification for 6 seconds, then centrifuged for 20 minutes at $1.3x10^5$ RPM at 4°C. Following the spindown, 50µL of each sample were set aside at -20°C for immunoblotting. 30µL of prepared Anti-FLAG® M2 Affinity Gel (Sigma-Aldrich) beads and 200µL of prepared Gluthathione Sepharose™ 4 Fast Flow beads (GE Healthcare) were added to each sample, then set to rotate for 2 hours at 4°C. Samples were then centrifuged at 6000 RPM for 2 minutes at 4°C, subsequently supernatant was discarded and the beads rinsed in 1mL of Co-IP buffer (minus protease inhibitor cocktail supplementation). Last step was repeated five times. Rinsed beads were resuspended in 20µL of TBS before adding to a SDS-PAGE gel for immunoblotting.

2.6 Protein Extraction and Immunoblotting

For protein extraction, cells were rinsed twice with PBS, then scraped from their wells using a cell lifter, transferred to an Eppendorf tube in PBS and centrifuged at $1.3x10^5$ RPM for 1 minute at room temperature. Supernatant was discarded, the cell pellets resuspended in 50 or 100µL of radioimmunoprecipitation assay (RIPA) lysis buffer (50mM Tris-HCl pH7.4, 1mM EDTA, 150mM NaCl, 1% NP-40, 0.5% SDS, and 0.5% Deoxycholic acid supplemented with either cOmplete™ Protease Inhibitor Cocktail (Sigma-Aldrich) or 1µM PMSF) and samples placed on ice for 30 minutes followed by 15 minutes centrifugation at $1.4x10^5$ RPM at 4°C. Supernatant was collected and the concentration of proteins were calculated using a Bradford assay.

30µg of protein lysates were mixed with ddH_2O and prepared 2X Laemmli Sample Buffer (Bio-rad) (supplemented with 5% β-mercaptoethanol), then set to migrate on a 10% or 12.5% SDS-PAGE gel. Electrophoresis was performed at 150 volts for 1 hour, then wet-transfer was performed for 1 hour at 100 volts onto 0.2µm Immun-Blot PVDF Membrane (Bio-Rad). Membranes were then probed for proteins using antibody conditions found in Table 2 of the Appendix.

Following the antibody incubation periods, membranes were rinsed with TBS or PBS, based on what was used during the antibody incubations, then incubated in Pierce® ECL Western Blotting Substrate (Thermo Scientific) to render the probed proteins visible once exposed onto HyBlot CL® Autoradiography Film (Denville) when developed using a Kodak X-OMAT 2000A processor.

2.7 *In-vitro* Kinase Assay

Kinase assays were performed using proteins purified as described above. Per sample, 2µg of substrate (or 10µL of affinity gel), 3µL of kinase buffer (200mM Tris-HCl pH7.5, 50mM β-Glycerolphosphate, ddH_2O, supplemented with 2mM $NaVO_4$ and 2.5µM DTT), 0.2µg of activated kinase (NUAK1, GST-tagged, Human, PRECISIO® Kinase, Recombinant, Sigma-Aldrich, Cat.# SRP5237) or 2µg of negative control protein, and up to 20µL of ddH_2O were combined. Samples were then mixed with 10µL of ^{32}P-ATP master mix (1µL Gamma ^{32}P-ATP (EasyTide, Perkin Elmer), 3µL 10X M-ATP (300µM ATP, 66mM $MgCl_2$, 33mM $MnCl_2$, ddH_2O), and 6µL ddH_2O). This mixture was then vortexed, centrifuged at $1.3x10^5$ RPM for 10 seconds, and incubated in the hybridization oven for 30 minutes at 30°C. 10µL of 4X SDS loading dye was added to the mix, gently vortexed, centrifuged, then boiled at 95°C for 3 minutes, after which the samples were centrifuged again. Samples were pipetted into the wells of a 10% or 12.5% SDS-PAGE gel, then

electrophoresis proceeded for 1 hour at 150 volts. Gels with samples were either dyed with Coomassie stain or wet-transferred onto a PVDF membrane as directed above. The stained gels or membranes were then sealed in cellophane, mounted onto a film cassette, along with a BioMax Transcreen High Energy Intensifying Screen (Kodak) and Amersham Hyperfilm™ ECL High Performance Chemiluminescence Film (GE Healthcare), then stored at -80°C for the desired time required to obtain visualization of bands (no longer than 24 hours).

2.8 Immunofluorescence and Confocal Microscopy

Cells were seeded onto sterilized coverslips (22x22mm, #1 thickness, VWR®) mounted in the wells of a 6 well culture plate. Once the desired experimental treatment was completed, the wells were rinsed once in PBS, then the coverslips were collected and set aside into a sterile 6 well culture plate for further treatment, while the remainder of the cells were collected for immunoblot analysis as described. Once removed, coverslips were fixed using a 3.7% formaldehyde solution (diluted in PBS) for 15 minutes with a gentle rocking, then rinsed with PBS. Subsequently, coverslips were incubated in a 0.2% Triton X-100 solution (diluted in PBS) for 5 minutes with a gentle rocking, then rinsed three times with PBS. Cells were then incubated in a 1% FBS solution (diluted in a Triton X-100/BSA buffer solution (0.2% BSA, 0.004% Triton X-100, PBS)) for 15 minutes with a gentle rocking, serving as the blocking agent, then stored at 4°C overnight. The following day, wells were incubated using the antibody conditions found in Table 3 of the Appendix. Wells were rinsed three times in PBS between antibody treatments and, while the secondary antibody was applied along with the following steps, the culture plate was wrapped in tinfoil to shield from exposure to light. Coverslips were finally treated with 1μg/mL of Hoechst 33342 solution (diluted in PBS) (Invitrogen) for 5 minutes with a gentle rocking. Coverslips were

then rinsed three times for 5 minutes with PBS and subsequently mounted onto Superfrost Microscope Slides (25x75x1.0mm, Fisher Scientific) using Dako Fluorescent Mounting Medium (Agilent), then set aside in a dark area to dry before applying a sealant over the edges of the coverslips. Images were taken using the Olympus 1X81 confocal microscope while using the 60X, water based, objective.

2.9 Kinetic Cell Imaging

Following the rescue experiment treatment, cells on the 6 well culture plates were rinsed once with PBS, then either 1.5mL of complete DMEM or 0.5M D-Sorbitol solution was added to the desired wells. Both complete DMEM and 0.5M D-Sorbitol solution were supplemented with the IncuCyte Caspase 3/7 Reagent for Apoptosis (Essen BioScience), at a dilution of 1:5000 from the stock. Using the IncuCyte^{TM} Zoom Live Kinetic Imaging System (Essen BioScience) and related software, green immunofluorescence was measured each hour over a period of 10 hours. Raw data was then exported and analysed via Microsoft Excel and GraphPad Prism 6 software.

2.10 ARK5 Drug Based Inhibition

Following the culturing and seeding of $2x10^5$ U2OS cells onto a 6 well culture plate mounted with coverslips (22x22mm, #1 thickness, VWR®) for 24 hours as discussed above in the cell culture section, cells were rinsed with PBS. As pre-treatment, each well was treated with either 2µL of DMSO or 2µL of WZ4003 (Tocris) (diluted in DMSO), final concentration of 10µM, diluted in 2mL of complete DMEM for 4 hours at 37°C with 5% CO_2. After which, cells were rinsed with PBS, then treated again with an identical amount of DMSO or drug diluted in either complete DMEM or 0.5M D-Sorbitol solution for 2 hours. Following the shock period, coverslips were

collected and treated as discussed in the immunofluorescence section and the remainder of the cells in the wells were collected using the manner discussed in the protein extraction protocol.

2.11 Statistical Analysis

Data collection for immunofluorescent images was performed using Columbus® image analysis program by cell counting. Caspase-3/7 analysis and data collection was performed using Essen BioScience IncuCyte Zoom kinetic cell imager and the related software. Densitometry of immunoblots was analysed using LI-COR® Image Studio software. Where appropriate, data was analysed using one-tailed, unpaired Student T-test with Welch's correction using the Graphpad Prism 6 software and are expressed as a mean ± standard error of mean of at least three independent experiments.

Chapter 3: Results

3.1 ARK5 plays a role in the subcellular localization of hnRNP A1 during hypertonic stress

Previously, a study was performed by the Holcik lab to determine possible kinases that are responsible for the relocalization of hnRNP A1 from the nucleus to the cytoplasm during hypertonic shock (Courteau *et al,* 2015). This data was obtained through an RNAi-based kinome wide screen using an arrayed library designed to target numerous genes related to the human kinome and was set as the base for this project (Figure 3.1 A and B). One of the hits of this screen, which was not characterized in the published paper, was ARK5 (Figure 3.1 C).

Therefore, the first goal of this project was to use two differently targeting siRNAs, which were not included in the original screen, to confirm the possible link between ARK5 and hnRNP A1. As shown in Figure 3.2 A and B, both siARK5#1 and siARK5#2 immunoblots depict the successful knockdown required to proceed with testing the hypothesis. Subsequently, using both variants of the siRNA, immunofluorescence was performed to visualize the location of hnRNP A1, both with and without hypertonic stress. In both cases, siRNA knockdown was shown to promote a nuclear localization phenotype of hnRNP A1 during stress (Figure 3.2 C and D). The analysis of repeated experiments determined that siARK5#1 caused an approximate 6 fold change reduction and ARK5#2 an approximate 5 fold change reduction in the cytoplasmic accumulation of hnRNP A1 when compared to the non-targeting control siRNA (Figure 3.2 E and F).

To further confirm the dependence of hnRNP A1 on ARK5 during hypertonic shock, an ARK5 rescue experiment was performed. Interestingly, the immunofluorescent images of this experiment

(Figure 3.3 A) and a quantification of repeated experiments (Figure 3.3 C), show a clear return to cytoplasmic accumulation of hnRNP A1 in osmotically shocked cells from the otherwise nuclear restriction that is seen in cells treated solely with the ARK5 siRNA. The levels of endogenous and overexpressed ARK5 are shown in Figure 3.3 B.

The experiment described above addressed the role of ARK5 protein levels in hnRNP A1 localization. In the subsequent experiment, I aimed to examine if the activity of ARK5 is needed to regulate hnRNP A1 shuttling. U2OS cells were therefore treated with the ARK5 pharmacological inhibitor WZ4003 prior to osmotic shock and the subcellular localization of hnRNP A1 was examined by confocal microscopy (Figure 3.4 A). I observed that although the levels of ARK5 were unchanged in cells treated with WZ4003 (Figure 3.4 B) the cytoplasmic accumulation of hnRNP A1 was attenuated to levels seen in siRNA treated cells (Figure 3.4 C). Altogether this data confirms that ARK5 activity is required for cytoplasmic accumulation of hnRNP A1 during hypertonic stress.

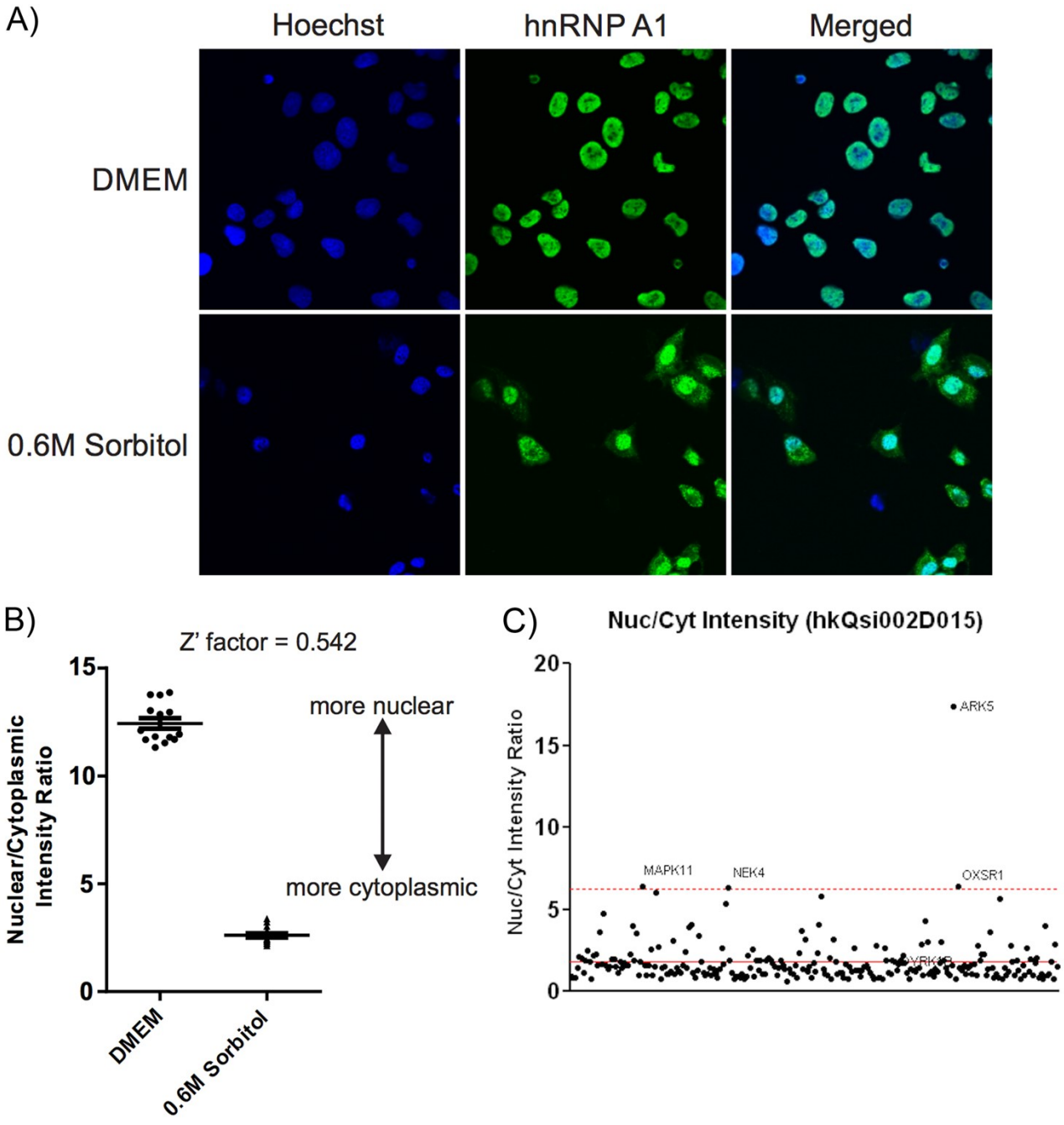
A)
Hoechst
hnRNP A1
Merged
DMEM
0.6M Sorbitol
B)
Z' factor = 0.542
Nuclear/Cytoplasmic Intensity Ratio
15
10
5
0
more nuclear
more cytoplasmic
DMEM
0.6M Sorbitol
C)
Nuc/Cyt Intensity (hkQsi002D015)
Nuc/Cyt Intensity Ratio
20
15
10
5
0
ARK5
MAPK11
NEK4
OXSR1

Figure 3.1: Results of RNAi-based kinome-wide screen identify ARK5 as a potential kinase which plays a regulatory role in hnRNP A1 accumulation mechanism during hypertonic shock. A) Representative immunofluorescence confocal microscopy images of U2OS cells treated with DMEM (top row) or a 0.6M sorbitol for 4 hours (bottom row). Nuclei were visualized using Hoechst staining. **B)** Graphical representation of A) depicting the nucleus vs. cytoplasmic intensity ratio of hnRNP A1 localization during the screen as determined by the analysis of the Z-factor. **C)** U2OS cells were reverse transfected using an arrayed library of siRNA pools designated to target 691 genes related to the human kinome for a period of 72 hours, followed by the induction of hypertonic shock via 0.6M sorbitol for 4 hours. The intensity ratios were calculated as in B) and plotted. Solid red line: mean of the plate; Red dashed line: 3σ. (Data modified from Courteau *et al,* 2015 for A and B).

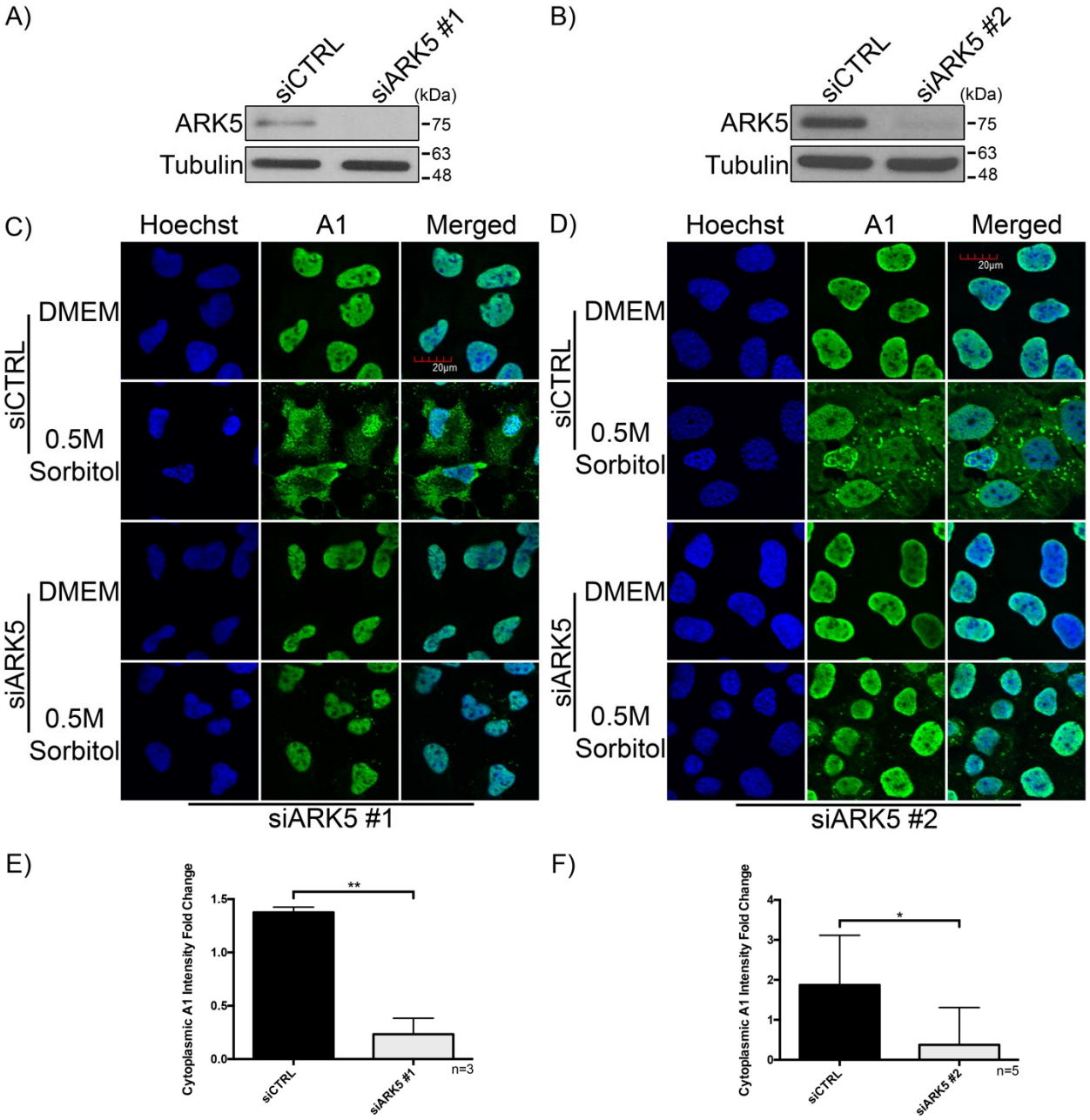
A)
siCTRL
siARK5 #1
(kDa)
ARK5
Tubulin
75
63
48
B)
siCTRL
siARK5 #2
(kDa)
ARK5
Tubulin
75
63
48
C)
Hoechst
A1
Merged
siCTRL
DMEM
0.5M Sorbitol
siARK5
DMEM
0.5M Sorbitol
20μm
siARK5 #1
D)
Hoechst
A1
Merged
siCTRL
DMEM
0.5M Sorbitol
siARK5
DMEM
0.5M Sorbitol
20μm
siARK5 #2
E)
Cytoplasmic A1 Intensity Fold Change
1.5
1.0
0.5
0.0
**
siCTRL
siARK5 #1
n=3
F)
Cytoplasmic A1 Intensity Fold Change
4
3
2
1
0
*
siCTRL
siARK5 #2
n=5

Figure 3.2: Cytoplasmic accumulation of hnRNP A1 is dependent on ARK5 during hypertonic shock. U2OS cells were transfected using two different site targeting, independent siRNAs for ARK5 to confirm results of the kinome-wide screen. **A)** and **B)** depict representative immunoblotting results of lysates from U2OS cells that had been transfected with either siARK5 (#1/#2) or a negative control siRNA (siCTRL) under normal physiological conditions. Tubulin was used as a loading control. **C)** and **D)** are representative immunofluorescence confocal microscopy images of U2OS cells treated for 2 hours with DMEM or a 0.5M sorbitol solution subsequent to the transfection. Nuclei were stained with Hoechst stain. Images were taken using the 60X, water based objective. Size marker shown in the top right image pertains to all images. **E)** and **F)** The quantification of replicates of C) and D) respectively, (*, $P<0.05$; **, $P<0.01$).

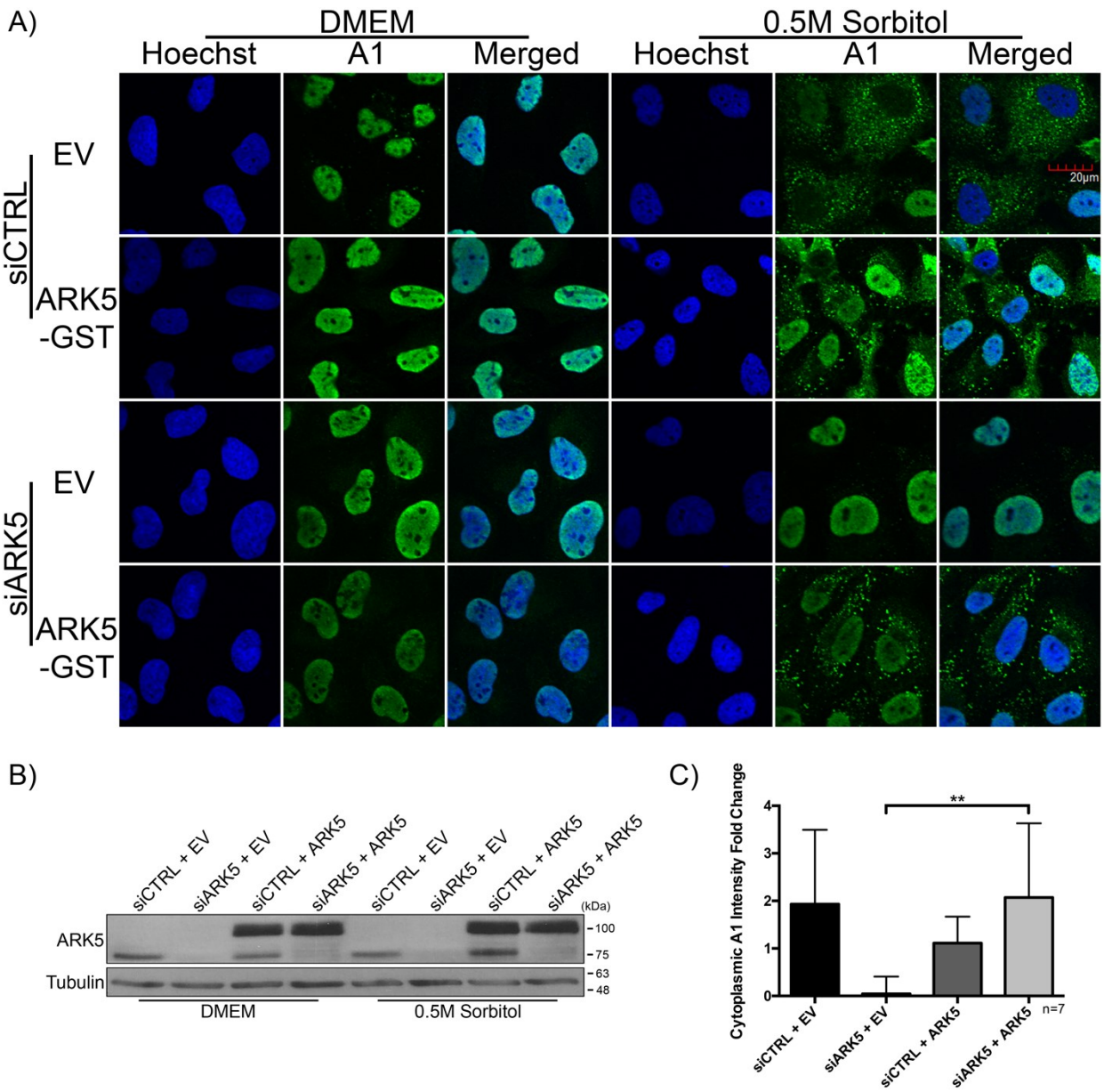
A)
DMEM
0.5M Sorbitol
Hoechst
A1
Merged
Hoechst
A1
Merged
siCTRL
EV
ARK5
-GST
siARK5
EV
ARK5
-GST
20μm
B)
siCTRL + EV
siARK5 + EV
siCTRL + ARK5
siARK5 + ARK5
siCTRL + EV
siARK5 + EV
siCTRL + ARK5
siARK5 + ARK5
(kDa)
ARK5
Tubulin
100
75
63
48
DMEM
0.5M Sorbitol
C)
Cytoplasmic A1 Intensity Fold Change
**
n=7
siCTRL + EV
siARK5 + EV
siCTRL + ARK5
siARK5 + ARK5

Figure 3.3: HnRNP A1 cytoplasmic accumulation is restored when ARK5 is overexpressed in U2OS cells previously transfected with siARK5. U2OS cells were transfected using a negative control siRNA (siCTRL) or siARK5, followed by transfection of a control plasmid (pmKate2-C) or a GST-tagged ARK5 plasmid (pDest27-ARK5) and subsequently treated with DMEM or 0.5M sorbitol. **A)** Representative immunofluorescence confocal microscopy images of treated U2OS cells. Nuclei were stained with Hoechst stain. Size marker shown in the top right image pertains to all images. **B)** Immunoblot confirmation of ARK5 knockdown and overexpression. **C)** Fold change quantification of cytoplasmic hnRNP A1 intensity found in A) for DMEM vs hypertonic shock treated cells, (**, $P<0.01$).

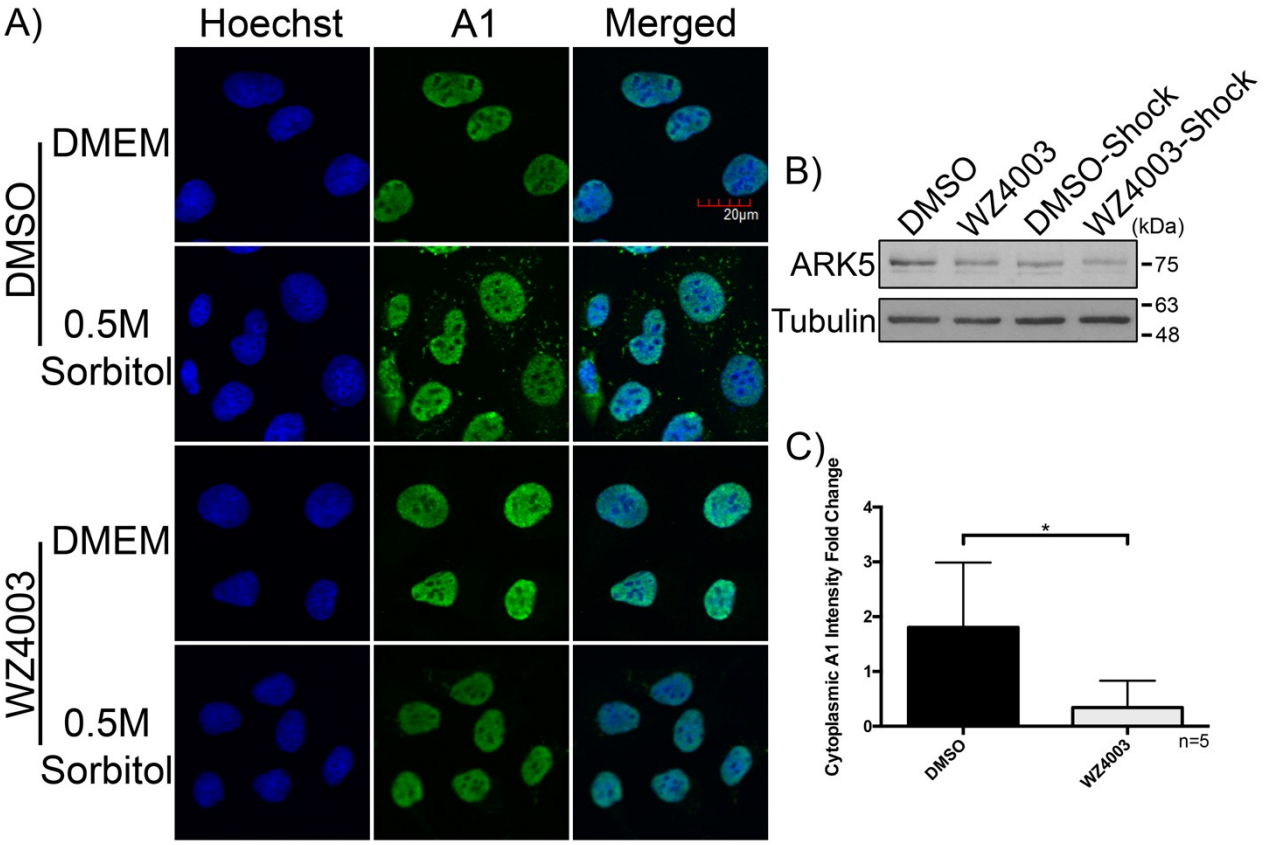
A)
Hoechst
A1
Merged
DMSO
DMEM
0.5M Sorbitol
WZ4003
DMEM
0.5M Sorbitol
20μm
B)
DMSO
WZ4003
DMSO-Shock
WZ4003-Shock
(kDa)
ARK5
Tubulin
75
63
48
C)
Cytoplasmic A1 Intensity Fold Change
*
DMSO
WZ4003
n=5

Figure 3.4: ARK5 inhibitor drug, WZ4003, inhibits cytoplasmic accumulation of hnRNP A1 during osmotic stress. U2OS cells were pre-treated with either DMSO or ARK5 inhibitor WZ4003, followed by a combination treatment of DMEM or 0.5M sorbitol including either DMSO or WZ4003. **A)** Representative immunofluorescence confocal microscopy images of treated U2OS cells. Nuclei were stained with Hoechst. Size marker shown in the top right image pertains to all images. **B)** U2OS cells lysates were subjected to immunoblotting with the indicated antibodies. **C)** Quantification of the repeated experiments from A (*, $P<0.05$).

3.2 ARK5 directly phosphorylates hnRNP A1 *in vitro*

It has been confirmed that hnRNP A1's accumulation within the cytoplasm is linked in part to the p38-mediated phosphorylation of serines found in the C-terminal F region of hnRNP A1 (Allemand *et al*, 2005). Having shown that ARK5 is required for the localization of hnRNP A1 during hypertonic stress, I next investigated whether ARK5 directly phosphorylates hnRNP A1. To do so, an *in vitro* kinase assay was performed using recombinant ARK5 and purified hnRNP A1 proteins from both eukaryotic and bacterial sources. GST-SAMS, a peptide shown previously to be phosphorylated by ARK5 (Suzuki *et al,* 2003) was used as a positive control while GST served as a negative control. I observed that FLAG-tagged hnRNP A1 purified from U2OS cells was robustly phosphorylated by ARK5 (Figure 3.5 A). To confirm that this phosphorylation is not due to an unknown protein that might have co-purified with hnRNP A1, a bacterially expressed His-tagged hnRNP A1 was used (Figure 3.5 B). Albeit faint, the signal for hnRNP A1 phosphorylation by ARK5 is present and thus confirms a direct phosphorylation of hnRNP A1 by ARK5.

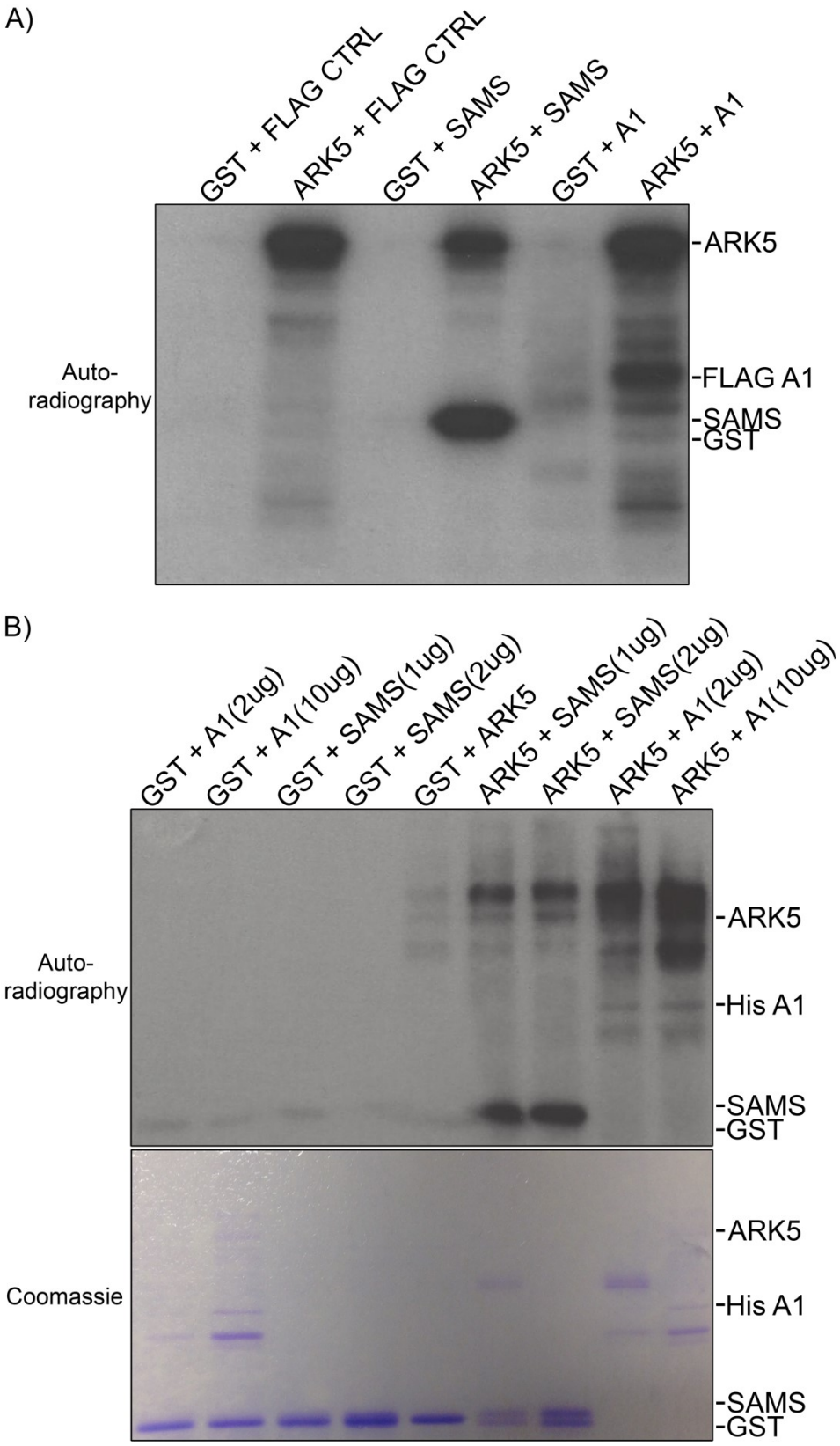
A)
GST + FLAG CTRL
ARK5 + FLAG CTRL
GST + SAMS
ARK5 + SAMS
GST + A1
ARK5 + A1
Auto-
radiography
-ARK5
-FLAG A1
-SAMS
-GST
B)
GST + A1(2ug)
GST + A1(10ug)
GST + SAMS(1ug)
GST + SAMS(2ug)
GST + ARK5
ARK5 + SAMS(1ug)
ARK5 + SAMS(2ug)
ARK5 + A1(2ug)
ARK5 + A1(10ug)
Auto-
radiography
-ARK5
-His A1
-SAMS
-GST
Coomassie
-ARK5
-His A1
-SAMS
-GST

Figure 3.5: ARK5 phosphorylates hnRNP A1 *in vitro*. A) U2OS cells were transiently transfected with FLAG expressing plasmid (negative control, FLAG CTRL) or WT FLAG-hnRNP A1 (A1) expressing plasmids, then FLAG-tagged proteins were immunoprecipitated, subjected to an *in vitro* kinase assay and separated by SDS-PAGE. **B)** BL21 cells were transfected with pTrcHis plasmid expressing hnRNP A1 and the bacterially expressed hnRNP A1 protein (A1) was isolated using His IMAC chromatography, subjected to an *in vitro* kinase assay and separated by SDS-PAGE. Recombinant GST-tagged SAMS peptide (SAMS) and GST were used as positive and negative controls, respectively.

3.3 ARK5 phosphorylates hnRNP A1 within the C-terminal part of the protein

With the confirmation of a direct phosphorylation of hnRNP A1 by ARK5, I aimed to identify which part of hnRNP A1 is phosphorylated. To accomplish this, the first attempt was to divide hnRNP A1 into three fragments containing different domains of the protein (Figure 3.6 A, middle row). Figure 3.6 B depicts the results of the *in vitro* kinase assay with these three fragments. Interestingly, none of these three fragments were phosphorylated. As it is possible that by splitting hnRNP A1 into three fragments a protein folding or a possible phosphorylation site was disrupted, I generated additional hnRNP A1 variants (Figure 3.6 A, bottom row) and tested them in an *in vitro* kinase assay (Figure 3.6 D). Only the protein containing the C-terminal half of the protein was phosphorylated under these conditions suggesting that the region required for phosphorylation by ARK5 was to be found between nucleotides 259 and 963.

To further identify the ARK5 phosphorylation site(s) on hnRNP A1 two approaches were used. First approach consisted of performing a sequence alignment between hnRNP A1 and a known ARK5 and AMPK substrate, synthetic SAMS peptide, which is often used as a positive control substrate for ARK5 and AMPK (Suzuki *et al,* 2003) to identify possible phosphorylation sites. This search identified one possible site (SASSS) which was used for further analysis. Based on this site, two mutants were produced, hnRNP A1 SASSS mutant 1 and 2, in which the serines were replaced by alanines. To generate the first mutant, site directed mutagenesis was used to make changes to the recombinant FLAG-hnRNP A1 plasmid's sequence which would result in the following mutations: S188A, S190A, and S191A. For producing hnRNP A1 SASSS mutant 2, primers were used to generate additional point mutations resulting in S192A using the hnRNP A1 SASSS mutant 1 sequence as the template. Despite expectations, neither of the two mutants

provided phosphorylation-null hnRNP A1 (Figure 3.7), suggesting that this region of hnRNP A1 is not involved in phosphorylation by ARK5. The second approach used previously identified regions of hnRNP A1, M9 and F that are known to play a role in hnRNP A1 localization (Allemand *et al*, 2005; Michael *et al*, 1995). Using recombinant proteins of these mutants of hnRNP A1, the loss of phosphorylation signal was observed only with the deletion of the M9 sequence (Figure 3.8 A). To further test if ARK5 and hnRNP A1 directly interact, I performed a co-immunoprecipitation experiment. I observed that both FLAG and GST purified cell lysates dual transfected with recombinant GST-ARK5 and FLAG-hnRNP A1, resulted in their co-purification. However, with the removal of hnRNP A1's M9 sequence, co-precipitation is reduced or absent. As a whole, this supports the notion that ARK5 interacts within the M9 sequence (amino acids 268-305) of hnRNP A1 and phosphorylates the C-terminal region of hnRNP A1.

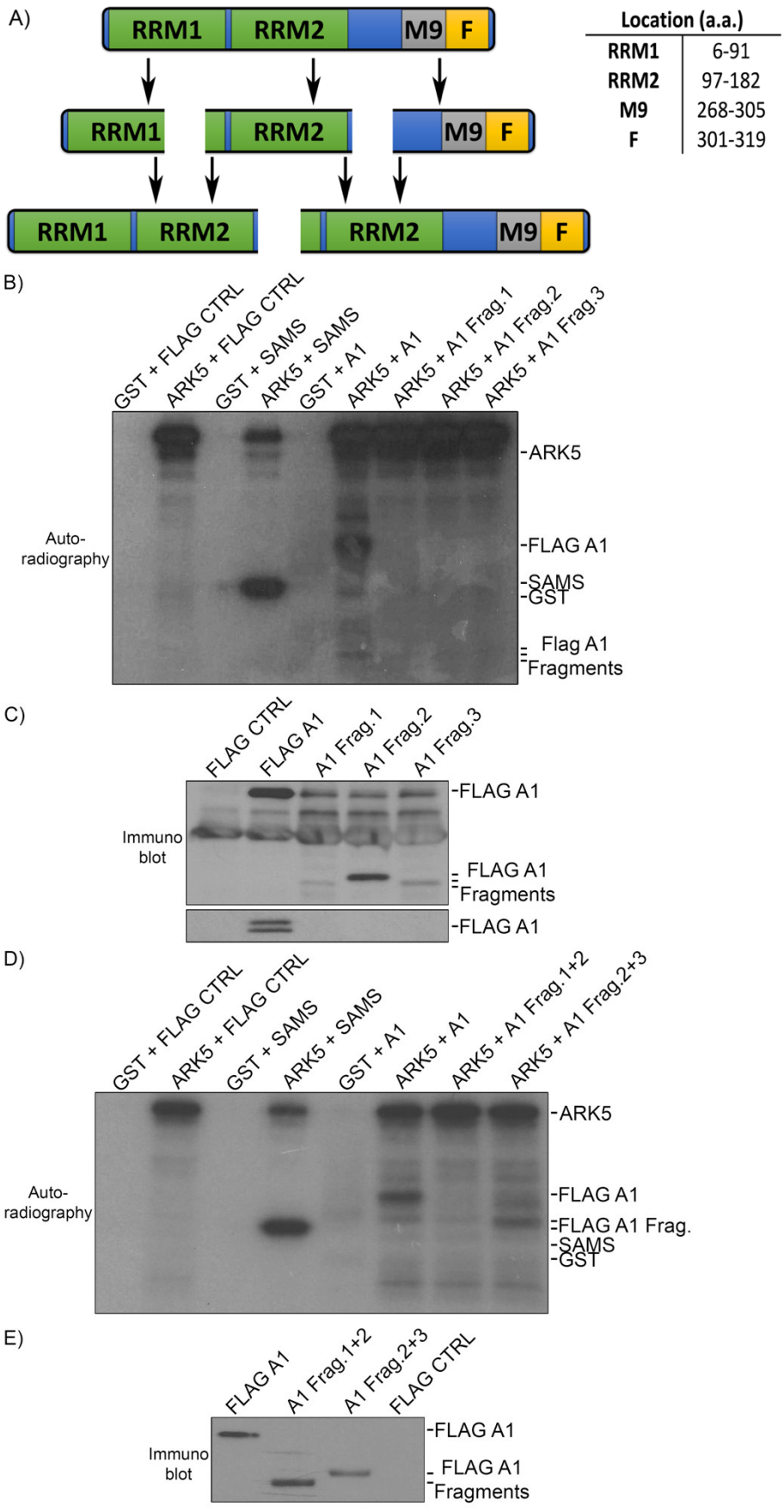
A)
RRM1
RRM2
M9
F
Location (a.a.)
RRM1 6-91
RRM2 97-182
M9 268-305
F 301-319
B)
GST + FLAG CTRL
ARK5 + FLAG CTRL
GST + SAMS
ARK5 + SAMS
GST + A1
ARK5 + A1
ARK5 + A1 Frag.1
ARK5 + A1 Frag.2
ARK5 + A1 Frag.3
Auto-radiography
-ARK5
-FLAG A1
-SAMS
-GST
-Flag A1 Fragments
C)
FLAG CTRL
FLAG A1
A1 Frag.1
A1 Frag.2
A1 Frag.3
Immuno blot
-FLAG A1
-FLAG A1 Fragments
-FLAG A1
D)
GST + FLAG CTRL
ARK5 + FLAG CTRL
GST + SAMS
ARK5 + SAMS
GST + A1
ARK5 + A1
ARK5 + A1 Frag.1+2
ARK5 + A1 Frag.2+3
Auto-radiography
-ARK5
-FLAG A1
-FLAG A1 Frag.
-SAMS
-GST
E)
FLAG A1
A1 Frag.1+2
A1 Frag.2+3
FLAG CTRL
Immuno blot
-FLAG A1
-FLAG A1 Fragments

Figure 3.6: Identification of ARK5 phosphorylation site(s) on hnRNP A1. A) Schematic diagram of hnRNP A1 deletion mutants used in kinase assay. Fragments are not shown to scale. **B)** and **D)** U2OS cells were transiently transfected with indicated FLAG-hnRNP A1 expressing plasmids (A1) and the FLAG-tagged proteins were immunoprecipitated, subjected to an *in vitro* kinase assay and separated by SDS-PAGE. (Fragment 1 [A1 Frag.1]: nucleotides 1-258, Fragment 2 [A1 Frag.2]: nucleotides 259-633, Fragment 3 [A1 Frag.3]: nucleotides 634-963, Fragment 1+2 [A1 Frag.1+2]: nucleotides 1-633, Fragment 2+3 [A1 Frag.2+3]: nucleotides 259-963). **C)** Immunoblotting of kinase assay samples done in parallel and probed for FLAG (above) and hnRNP A1 (below). **E)** Immunoblotting of kinase assay samples done in parallel and probed for FLAG.

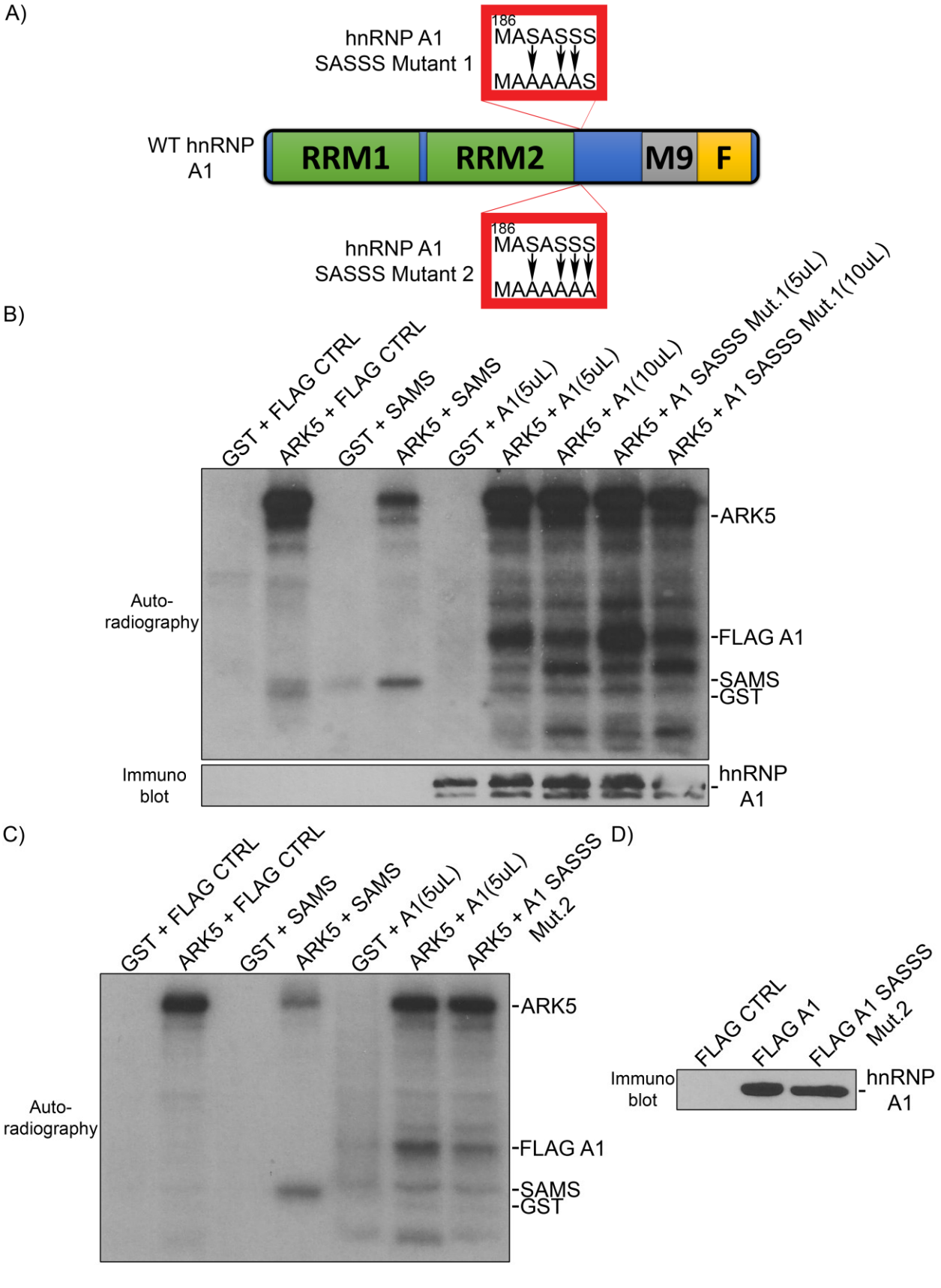
A)
hnRNP A1
SASSS Mutant 1
186
MASASSS
MAAAAAS
WT hnRNP
A1
RRM1
RRM2
M9
F
hnRNP A1
SASSS Mutant 2
186
MASASSS
MAAAAAA
B)
GST + FLAG CTRL
ARK5 + FLAG CTRL
GST + SAMS
ARK5 + SAMS
GST + A1(5uL)
ARK5 + A1(5uL)
ARK5 + A1(10uL)
ARK5 + A1 SASSS Mut.1(5uL)
ARK5 + A1 SASSS Mut.1(10uL)
Auto-
radiography
-ARK5
-FLAG A1
-SAMS
-GST
Immuno
blot
-hnRNP
A1
C)
GST + FLAG CTRL
ARK5 + FLAG CTRL
GST + SAMS
ARK5 + SAMS
GST + A1(5uL)
ARK5 + A1(5uL)
ARK5 + A1 SASSS
Mut.2
Auto-
radiography
-ARK5
-FLAG A1
-SAMS
-GST
D)
FLAG CTRL
FLAG A1
FLAG A1 SASSS
Mut.2
Immuno
blot
-hnRNP
A1

Figure 3.7: Identification of ARK5 phosphorylation site(s) on hnRNP A1 via mutagenesis. **A)** Schematic diagram of hnRNP A1 site directed mutagenesis mutants used in kinase assay (FLAG-hnRNP A1 SAMS mutant, S188A, S190A, S191A; FLAG-hnRNP A1 SASSS mutant, S188A, S190A, S191A, S192A). Not shown to scale**. B)** and **C)** U2OS cells were transiently transfected with WT or mutant FLAG-hnRNP A1 expressing plasmids, then FLAG-tagged proteins were immunoprecipitated and subjected to an *in vitro* kinase assay and separated by SDS-PAGE. **B)** Immunoblotting of kinase assay's membrane probed for hnRNP A1 (below). **D)** Immunoblotting of kinase assay samples done in parallel and probed for FLAG.

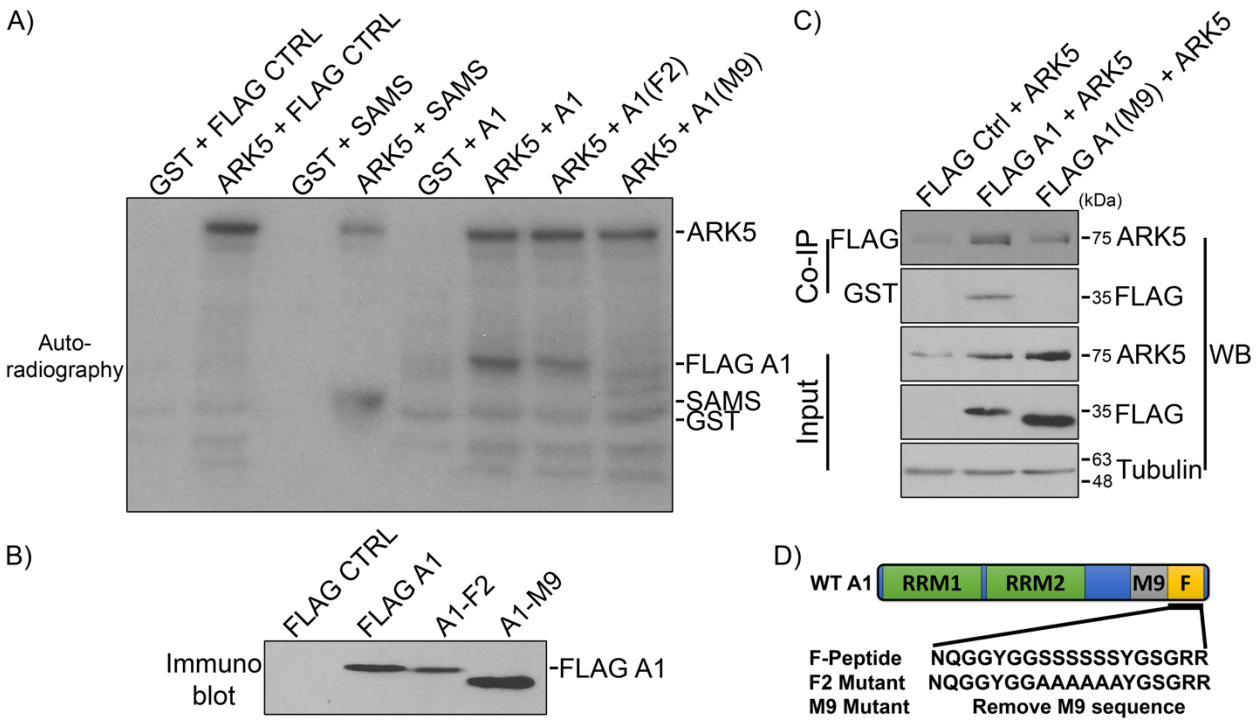
A)
GST + FLAG CTRL
ARK5 + FLAG CTRL
GST + SAMS
ARK5 + SAMS
GST + A1
ARK5 + A1
ARK5 + A1(F2)
ARK5 + A1(M9)
Auto-radiography
ARK5
FLAG A1
SAMS
GST
B)
FLAG CTRL
FLAG A1
A1-F2
A1-M9
Immuno blot
FLAG A1
C)
FLAG Ctrl + ARK5
FLAG A1 + ARK5
FLAG A1(M9) + ARK5
(kDa)
Co-IP
FLAG
GST
Input
75 ARK5
35 FLAG
75 ARK5
35 FLAG
63
48 Tubulin
WB
D)
WT A1
RRM1
RRM2
M9
F
F-Peptide NQGGYGGSSSSSSYGSGRR
F2 Mutant NQGGYGGAAAAAAYGSGRR
M9 Mutant Remove M9 sequence

Figure 3.8: ARK5 phosphorylation site on hnRNP A1 is potentially linked to the M9 sequence. A) U2OS cells were transiently transfected with indicated FLAG-hnRNP A1 expressing plasmids (A1) or FLAG-tagged hnRNP A1 mutants (FLAG-hnRNP A1-F2 and FLAG-hnRNP A1-ΔM9) and the FLAG-tagged proteins were immunoprecipitated, subjected to an *in vitro* kinase assay and separated by SDS-PAGE. **B)** Immunoblotting of kinase assay samples done in parallel and probed for FLAG. **C)** Co-immunoprecipitation of U2OS cells transfected with FLAG-expressing plasmid (FLAG Ctrl), FLAG-tagged hnRNP A1 (FLAG A1), FLAG-tagged hnRNP A1-ΔM9 (FLAG A1 (M9)), and GST-tagged ARK5 (ARK5). First row shows proteins immunoprecipitated using FLAG affinity gel and probed for ARK5. Second row depict proteins immunoprecipitated via GST affinity gel and probed for FLAG. Input is shown at the bottom. Tubulin was used as a loading control. **D)** Schematic diagram of changes occurred in hnRNP A1 F2 and ΔM9 mutants. Fragments are not shown to scale.

3.4 ARK5-dependent localization of hnRNP A1 regulates expression of Bcl-xL

Having confirmed that hnRNP A1's phosphorylation and the subsequent cytoplasmic accumulation is dependent on ARK5 within a cell, the protein levels of the downstream target of hnRNP A1, Bcl-xL, were measured. Bcl-xL is ideal as supporting research shows that cytoplasmic hnRNP A1, induced by osmotic shock, regulates the selective IRES-based translation of Bcl-xL as a response to the stress (Bevilacqua *et al*, 2010). Determined by immunoblotting, results show that siRNA mediated knockdown of ARK5 leads to the concomitant increase of Bcl-xL (Figure 3.9 A), an increase noticed also when cells are hypertonically shocked (Figure 3.9 B). Furthermore, Bcl-xL's presence within osmotically stressed cells is further increased by 78% when also treated with siARK5, an increase which is reversed with the subsequent rescue of exogenous ARK5. Overall, this demonstrates a link between ARK5 dependent localization of hnRNP A1 and the expression of Bcl-xL.

As the previous experiment served to identify the link between ARK5's regulatory role of hnRNP A1's selective translation of Bcl-xL, with the following experiment I aimed to use hnRNP A1 mutants that targets specifically the localization mechanism, previously identified in literature, to exclude the possibility of hnRNP A1's localization or the presence of ARK5 having an individual effect towards Bcl-xL. Using nucleus and cytoplasm restricted mutants, FLAG-hnRNP A1 F2 and FLAG-hnRNP A1 ΔM9 (Figure 3.10 B), Bcl-xL was observed to show a plausible trend leading to an increase in protein levels while hnRNP A1 was restricted to the nucleus and, by comparison, a decrease if hnRNP A1 was constrained to the cytoplasm. However, the differences were not statistically discernable.

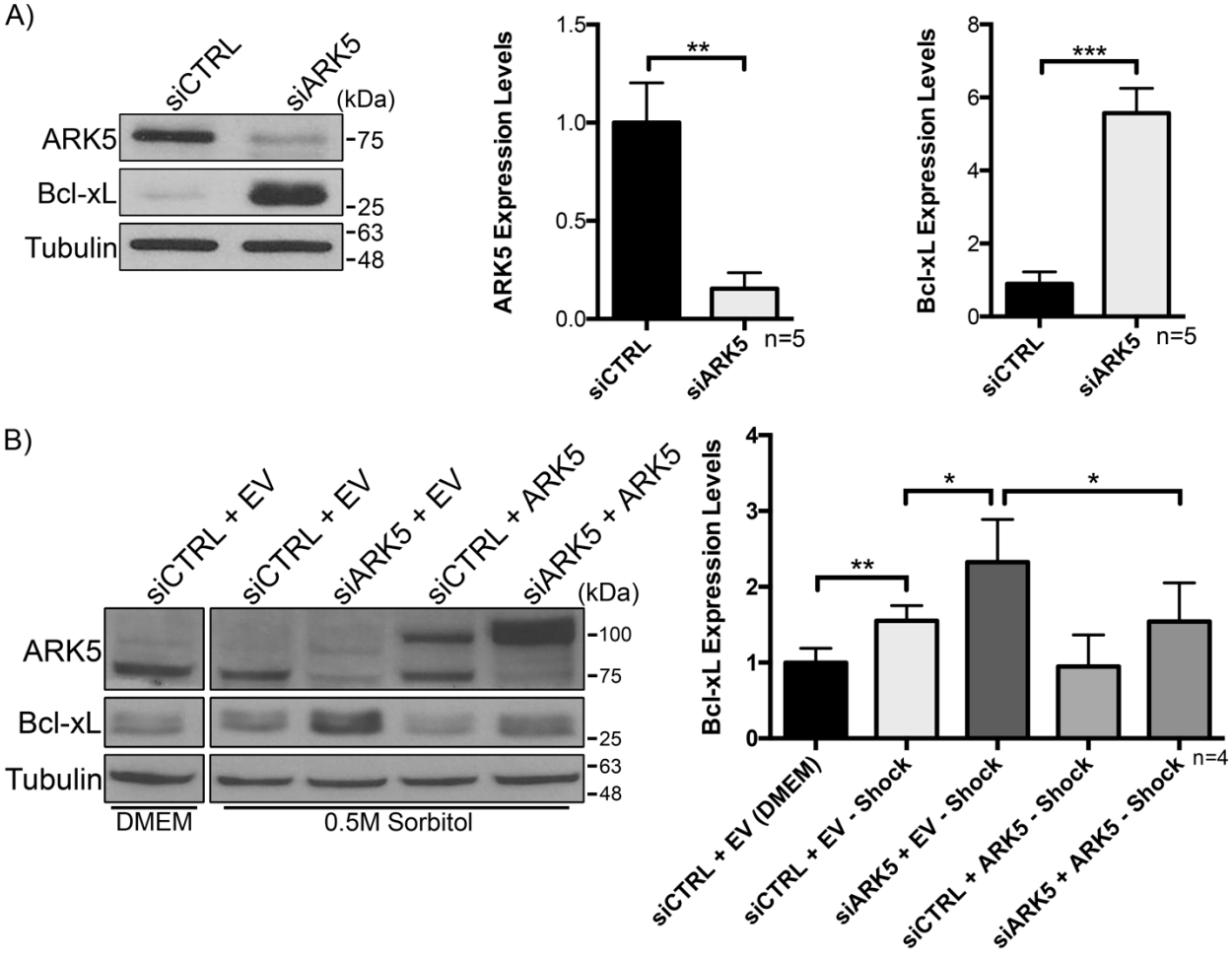
A)
siCTRL
siARK5
(kDa)
ARK5
Bcl-xL
Tubulin
75
25
63
48
ARK5 Expression Levels
**
n=5
Bcl-xL Expression Levels
***
n=5
B)
siCTRL + EV
siCTRL + EV
siARK5 + EV
siCTRL + ARK5
siARK5 + ARK5
(kDa)
ARK5
Bcl-xL
Tubulin
100
75
25
63
48
DMEM
0.5M Sorbitol
Bcl-xL Expression Levels
**
*
*
n=4
siCTRL + EV (DMEM)
siCTRL + EV - Shock
siARK5 + EV - Shock
siCTRL + ARK5 - Shock
siARK5 + ARK5 - Shock

Figure 3.9: Expression of Bcl-xL, a known target of hnRNP A1, is controlled by ARK5 through hnRNP A1's subcellular localization during hypertonic stress. U2OS cells were transfected using siCTRL (negative control) or siARK5 and in B) followed by a transfection of plasmid DNA of a control plasmid (EV) or a GST-tagged ARK5 plasmid (ARK5). **A)** Representative immunoblot (left) and densitometry from repeated experiments (right) of ARK5 and Bcl-xL levels of cells grown in DMEM and transfected with siRNA. **B)** Representative immunoblot (left) and densitometry data from repeated experiments (right) of cells grown in 0.5M sorbitol during an ARK5 rescue (normalized to siCTRL + EV (DMEM)). Tubulin was used as a loading control (*, $P<0.05$; **, $P<0.01$).

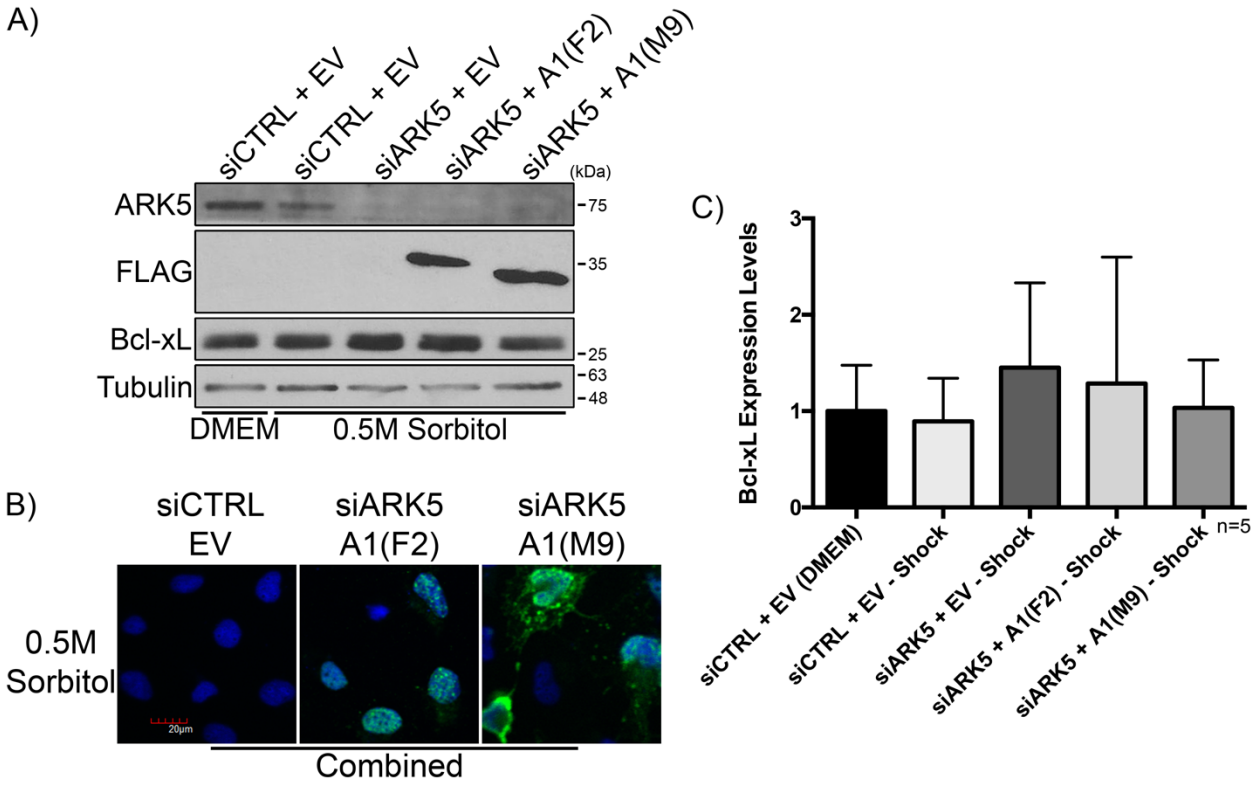
A)
siCTRL + EV
siCTRL + EV
siARK5 + EV
siARK5 + A1(F2)
siARK5 + A1(M9)
(kDa)
ARK5
FLAG
Bcl-xL
Tubulin
75
35
25
63
48
DMEM
0.5M Sorbitol
B)
siCTRL EV
siARK5 A1(F2)
siARK5 A1(M9)
0.5M Sorbitol
20μm
Combined
C)
Bcl-xL Expression Levels
0
1
2
3
n=5
siCTRL + EV (DMEM)
siCTRL + EV - Shock
siARK5 + EV - Shock
siARK5 + A1(F2) - Shock
siARK5 + A1(M9) - Shock

Figure 3.10: Restricting hnRNP A1 to the nucleus or the cytoplasm shows a possible link to controlling Bcl-xL levels. U2OS cells were transfected using siCTRL (negative control) or siARK5, followed by a transfection of plasmid DNA of a control plasmid (EV), or FLAG-tagged hnRNP A1 mutants (FLAG-hnRNP A1-F2 or FLAG-hnRNP A1-ΔM9). **A)** Representative immunoblot of endogenous ARK5, Bcl-xL and transfected hnRNP A1 protein levels. Tubulin was used as a loading control. **B)** Representative immunofluorescent confocal images of hypertonically shocked U2OS cells with either a negative control or hnRNP A1 mutant overexpression following a siRNA transfection. Cells were probed for FLAG and nuclei visualized using Hoechst stain. Size marker shown in the left image pertains to all images. **C)** Quantification of replicates of experiments measuring Bcl-xL levels found in cells with or without the presence of stress during the restriction of hnRNP A1 localization.

3.5 Removal of ARK5 leads to increased vitality in stressed U2OS cells

Having previously confirmed a link between the anti-apoptotic Bcl-xL, hnRNP A1 and ARK5, I aimed to observe the potential of manipulating this pathway to mediate a change in the viability of stressed cells. This approach concerned using live cell imaging to measure the relative changes in the activation of caspases 3 and 7 over a 10 hour period. Interestingly, observations showed that caspases 3 and 7 activation for stressed cells took three to four hours before showing any noticeable increase in cells with unaltered levels of endogenous ARK5. In contrast, cells transiently transfected with siARK5 showed that caspases 3 and 7 activation was delayed until the seven to eight hour time point. In addition to this delay, cells solely treated with siARK5 showed greater decreased levels of caspase activation, whereas activation escalated following exogenous ARK5 transfection. In short, these results confirm a link between ARK5's regulation of hnRNP A1's subcellular localization and the onset of cell death markers.

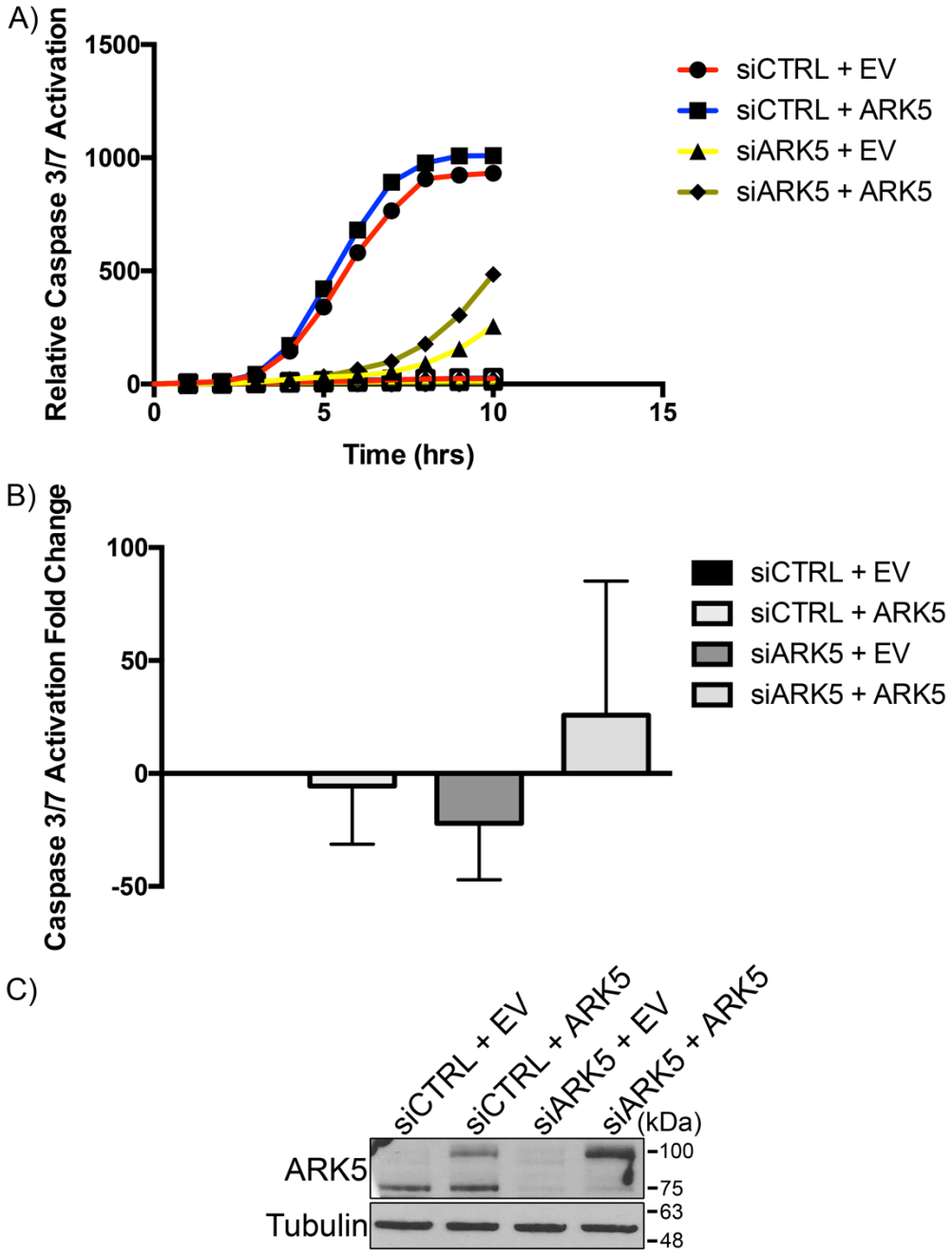
A)
Relative Caspase 3/7 Activation
1500
1000
500
0
0
5
10
15
Time (hrs)
siCTRL + EV
siCTRL + ARK5
siARK5 + EV
siARK5 + ARK5
B)
Caspase 3/7 Activation Fold Change
100
50
0
-50
siCTRL + EV
siCTRL + ARK5
siARK5 + EV
siARK5 + ARK5
C)
siCTRL + EV
siCTRL + ARK5
siARK5 + EV
siARK5 + ARK5
(kDa)
ARK5
Tubulin
100
75
63
48

Figure 3.11: Knockdown of ARK5 results in an increased resistance to hypertonic stress. U2OS cells were transiently transfected with siCTRL, siARK5, negative control plasmid or GST-tagged ARK5 and subsequently treated with 0.5M sorbitol. **A)** Quantification of caspase 3 and 7 activation in which the y-axis depicts the sum of fluorescent cells normalized to the percentage of cell confluency. Hollow shapes portray data of samples cultured in DMEM and solid for those maintained in 0.5M sorbitol during the 10 hours monitored. **B)** Representation of the difference in fold change between siCTRL-EV and the other treatment conditions at the 10 hour time point. 16 images were taken from each well. **C)** Representative immunoblot of A) using samples gathered in parallel. Tubulin was used as a loading control.

Chapter 4: Discussion

The onset and prolonged exposure of stress, in this case hypertonic stress, can lead to both biochemical and physical changes in a cell, one of which is the subcellular relocalization of hnRNP A1, noted to be due to the phosphorylation of its C-terminus region (Allemand *et al*, 2005). This response, in part, is what allows a cell to overcome the attenuation of cap-dependent translation, caused by the stress, by switching to IRES-mediated translation to produce or inhibit proteins required to potentiate a recovery or ensure cell death while undergoing stress (Fernandez *et al*, 2002). Although the phenotype of hnRNP A1's cytoplasmic accumulation is found to be replicated in various cell types, the exact mechanism by which this comes about is still not fully understood. However, based on previously performed research, a list of potential kinase regulators of hnRNP A1's shuttling activity have been identified (Figure 3.1) (Allemand *et al*, 2005; Bevilacqua *et al*, 2010; Courteau *et al,* 2015; Roy *et al,* 2014). From this list, the serine/threonine kinase ARK5 is considered for its potential as the regulator of hnRNP A1's subcellular location by phosphorylation in response to hypertonic stress along with its potential cascading downstream effects on known targets of hnRNP A1.

In this study, I sought to identify the importance of ARK5 in the localization of hnRNP A1 during hypertonic stress. To do so, I aimed first to validate the results of the RNAi kinome-wide screen, through which ARK5 was identified. By performing siRNA mediated knockdown using two independent siRNAs, different to those used in the original screen, it was found that the loss of ARK5 coincided with the loss of hnRNP A1 cytoplasmic accumulation in the presence of stress and hnRNP A1 displayed clear signs of major nuclear accumulation (Figure 3.2). Therefore, replicating the results found via the initial screen. In addition to this, the two siRNAs where used

to exclude the possibility of off-targeting effects, an occurrence often seen in larger RNAi screens (Sigoillot and King, 2011), which, in turn, further proposes that specific knockdown of ARK5 results in the nuclear accumulation of hnRNP A1. Taking this as an indication towards the importance of ARK5 to the mechanism, further testing was assessed by an ARK5 rescue experiment, to which the results showed that by restoring endogenous levels of ARK5 subsequent to its knockdown, cytoplasmic accumulation is concomitantly returned when stress is present (Figure 3.3). Interestingly, the cytoplasmic accumulation of hnRNP A1 is only shown to be affected if ARK5 levels are restored after having been lowered via siRNA, as solely increasing the amount of ARK5, beyond endogenous levels, did not significantly alter the cytoplasmic accumulation. Despite the initial conception that a related increase in the cytoplasmic response would correlate with the increase of ARK5, I propose this could have been due to hnRNP A1 having reached a plateau in terms of its presence within the cytoplasm or with the quantity of possible hnRNP A1 phosphorylated proteins. As such, further increasing endogenous levels of ARK5 does not insight the opposite reaction to its reduction. Overall, these two experiments confirm that hnRNP A1's cytoplasmic accumulation is due to the presence of ARK5. However, ARK5 is not the only kinase that has been identified as a regulator of hnRNP A1's localization. In addition to ARK5, the removal of either HK2 or MAPK11 have been shown to cause the loss of hnRNP A1's cytoplasmic accumulation (Courteau *et al,* 2015). As this is the case, it is possible that in some way these three kinases could be exposed to genetic interplay to resolve the relocalization of hnRNP A1 during hypertonic stress. However, of these three kinases, ARK5 is the first to have been identified as directly interacting with hnRNP A1 and further testing will be necessary to confirm a possible link between these three kinases. A link which could be hierarchical in nature or could provide insight to communication between their individual

signalling pathways. It is also possible that these kinases are activated by different upstream signals and could eventually go on to affect different regions of hnRNP A1. In addition, drug based inhibition of ARK5 was also assessed to determine if ARK5's presence or activity alone alters the stress induced cytoplasmic accumulation of hnRNP A1. As such, WZ4003 was chosen due to its reported high specificity towards ARK5 at a low IC50 (Banerjee *et al*, 2014a). This experiment showed that when pre-treated, similar tendencies to reduce the cytoplasmic accumulation occurred, mimicking that which is seen during the knockdown method (Figure 3.4), therefore suggesting that hnRNP A1's subcellular localization is not only dependent on ARK5's presence, but also on ARK5's activity.

The evidence above confirms the link between ARK5 and hnRNP A1's subcellular localization. However, this data lacks details as to how ARK5 regulates hnRNP A1, be it by means of a direct or indirect phosphorylation. To address the inquiry towards ARK5's potential to directly phosphorylate hnRNP A1, an *in vitro* kinase assay was performed using recombinant ARK5 and hnRNP A1 purified from eukaryotic and bacterial sources. Based on the results, we can conclude that the robust signal observed while using eukaryotically expressed FLAG-tagged hnRNP A1 suggests a direct interaction between ARK5 and hnRNP A1 (Figure 3.5 A). Conversely, one of the limitations of proteins purified from eukaryotic sources is the possibility of a co-precipitation pulldown of an unwanted, secondary protein attached to the protein of interest, which could serve to provide a false positive in the assay (Kaboord and Perr, 2008). To overcome the downfall of this method and to provide a secondary confirmation to the proposed direct interaction, the kinase assay was repeated using bacterially sourced His-tagged hnRNP A1. Intriguingly, through this assay, phosphorylation was observed a second time, albeit, the magnitude of the perceived results

appeared faint in comparison to the phosphorylated FLAG-tagged hnRNP A1. In regards to the faint band found when using His-tagged hnRNP A1, I propose this could be due to the lack of post-translational modification(s) the recombinant protein would typically undergo when expressed from a eukaryotic source, which resulted in the reduced interaction and that this, by extension, could explain the difference in the robust expression observed in the first kinase assay.

Having now, discerned that hnRNP A1 is directly phosphorylated by ARK5, I then questioned the site of phosphorylation by dividing hnRNP A1 into three fragments (Figure 3.6, middle row). Remarkably, the use of the three fragments resulted in no observable phosphorylation, despite hnRNP A1 previously showing this capability when whole (Figure 3.6 B). As such, I believe this loss of phosphorylation could be due to the smaller size of the fragments, therefore possibly resulting in the loss of the three-dimensional conformation required for the kinase to bind to the substrate. To add to this, the loss of phosphorylation could have instead been the result of the site of interaction for ARK5 being spilt between two of the fragments. Therefore, to exclude these possibilities, two larger variants of the fragments were generated (Figure 3.6 A, bottom row) and subsequently tested for their ability to be phosphorylated by ARK5. As it turns out, phosphorylation occurred using the larger variants and from this, I concluded that phosphorylation takes part somewhere between nucleotides 259 and 963.

Based on the presumption that the site of interaction and phosphorylation were found to be somewhere within the C-terminal portion of hnRNP A1, mutants where generated considering possible targets within the proposed area of effect with the goal of generating phosphorylation-null versions of hnRNP A1 by inhibiting ARK5's interaction. The first series of mutants were

generated based on a DNA alignment performed between hnRNP A1 and a well-known positive substrate of ARK5, the SAMS peptide (Suzuki *et al,* 2003). Via this alignment, one possible site (SASSS) was identified and used for further testing. The hnRNP A1 SASSS mutant 1 was generated from this site by performing serine-to-alanine mutations at three sites, while a fourth serine was altered in mutant 2 due to its proximity to the site of interest and that research shows previous history of this serine being phosphorylated by Mnk1, albeit under different conditions (Buxadé *et al,* 2005) (Figure 3.7 A). Despite the preconceptions due to their similarity with the SAMS peptide, these two mutants were observed to be phosphorylated. However, I propose one reason that these mutants did not produce the intended results, is due to the difference in sequence between hnRNP A1's proposed site of interest and the SAMS peptide. In addition, ARK5 has been noted in literature to phosphorylate, but is not limited to, the following proteins: caspase 6, phosphorylated at Ser257; and p53, phosphorylated at Ser15 and Ser392 (Hou *et al,* 2011; Suzuki *et al,* 2004). Interestingly, upon further study of the sequences surrounding these phosphorylation sites, it is discerned that none of the surrounding sequences are similar. As this is the case, I propose that utilizing only previously determined sequences as a guide to determine the potential site of interest of ARK5 for hnRNP A1 could prove to become rather difficult and would require further study.

For the second site, both FLAG-tagged hnRNP A1 F2 and ΔM9 mutants were considered for the possible site of interaction, based on research having previously identified their link to the localization of hnRNP A1 and their related phosphorylation (Allemand *et al*, 2005; Michael *et al*, 1995). In using these two mutants of hnRNP A1, phosphorylation was observed for the F2 variant, however phosphorylation is lost along with the elimination of the M9 sequence. This data serves

to further isolate the phosphorylation site of ARK5 and, by extension, again supports the importance of the M9 sequence to the mechanism discussed. In conjunction with the kinase assay, an attempt was made to further confirm the relation between the M9 sequence and ARK5 by examining the loss of binding with an attempted co-immunoprecipitation by targeting the two tags used in either of the recombinant proteins (Figure 3.8 C). In support of the above stated findings, the results show a clear binding between hnRNP A1 WT and ARK5, however, by removing the M9 sequence, the quantity of the attached secondary protein is reduced or absent and therefore this could be concluded as a correlation to the loss of interaction. In summary, the interaction site for ARK5 has been narrowed down to the M9 region of hnRNP A1. Although, as the exact phosphorylation site has yet to be determined, I propose that by using the previously identified ARK5 target sequences of other proteins, this method could serve to later provide the exact phosphorylation site(s) that could reside within the M9 sequence. To further expand upon this mechanism, the interaction between kinase and substrate can be performed through two mechanisms. One which allows the kinase to directly bind to the site of phosphorylation, while the other employs a docking mechanism in which the kinase binds to a region other than the imposed phosphorylation site (Reményi *et al,* 2006). Based on the observed results, where ARK5 interacts with the M9 sequence, the mechanism of action could employ the M9 sequence as the docking site for ARK5 or it could be explained with ARK5 directly targeting a serine(s) located within the M9 sequence. As with previous kinases that phosphorylate hnRNP A1, there lies the possibility that phosphorylation can occur within the regions that play roles in the localization mechanism or within a different area, yet still affect hnRNP A1's location. To support this, there is research having confirmed that, during osmotic shock, when the $(MKK)_{3/6}$-p38 signaling pathways is activated, phosphorylation of the F-peptide is performed by Mnk1/2 resulting in hnRNP A1

cytoplasmic accumulation, while, under different conditions, S6K2 phosphorylates serine 4, outside of the M9 region, and aids hnRNP A1's nuclear export (Allemand *et al*, 2005; Roy *et al,* 2014). Overall, my results have only shown that M9 is necessary for the interaction between ARK5 and hnRNP A1 and further study will be needed to confirm ARK5's targeted phosphorylation site(s).

HnRNP A1 is an RNA binding protein known for many roles pertaining to protein synthesis and RNA metabolism, to which one of importance to this study is its role as an ITAF to regulate the synthesis of select proteins, particularly those that concern the mRNAs of proteins related to pro and anti-apoptotic functions. Previously, hnRNP A1 has been identified as an ITAF for the following mRNA: XIAP, Apaf-1, HRV, and Bcl-xL (Bevilacqua *et al*, 2010; Cammas *et al,* 2007; Lewis *et al,* 2007). As such, to further validate and study the extent of how ARK5 affects hnRNP A1, I investigated the changes in hnRNP A1's target gene expression, in this case Bcl-xL, through the effects of ARK5 mediated localization of hnRNP A1. Previous research has confirmed that hypertonic stress induced cytoplasmic accumulation of hnRNP A1 ultimately inhibits the expression of Bcl-xL (Bevilacqua *et al*, 2010). Therefore, I had proposed that with the removal of ARK5, hnRNP A1 would no longer accumulate within the cytoplasm and its absence would be accompanied by an increase of Bcl-xL proteins. As such, an increase in Bcl-xL levels is what was observed under non-shock conditions (Figure 3.9 A). However, despite that Bcl-xL is described as decreased due to hypertonic shock, in contradiction I observed that during my imposed shock conditions, Bcl-xL protein levels are increased (Figure 3.9 B). Remarkably, what has been previously described about Bcl-xL expression during hypertonic stress is not as simple as an immediate decrease. In fact, data shows that through exposure to hypertonic stress and concomitant

cytoplasmic accumulation of hnRNP A1, Bcl-xL increases during early time points, but will dissipate over the next several hours (Bevilacqua *et al*, 2010). Consequently, the increase in Bcl-xL protein levels observed during the hypertonic stress conditions in this study is in accordance with previously observed data (Bevilacqua *et al*, 2010). In addition to this increase during hypertonic stress, the expression of Bcl-xL is yet again increased with the removal of ARK5 (Figure 3.9 B). Interestingly, by performing a rescue expression of ARK5, the noted increase observed during ARK5's absence is no longer present and Bcl-xL protein levels show an expression similar to that which is seen in unaltered U2OS cells during hypertonic stress. As a whole, these variations in Bcl-xL protein levels in response to the presence of ARK5 confirms that ARK5 plays a regulatory role in altering the expression of a hnRNP A1 target gene through hnRNP A1's phosphorylation and localization.

As it has been determined that cytoplasmic and not nuclear hnRNP A1 is the cause of alteration to IRES-mediated translation (Cammas *et al,* 2007), in extension of the previous experiment, cells were transfected with either the nuclear or cytoplasmic mutants of hnRNP A1, F2 or ΔM9, to confirm that it is not solely ARK5's presence or hnRNP A1's subcellular localization that leads to the observed altered levels of Bcl-xL. Intriguingly, this experiment showed no significant changes between the conditions (Figure 3.10 C). Upon further observations, I propose that this is due to the observable lack of total nuclear and cytoplasmic accumulation when using the mutants (Figure 3.10 B). By immunofluorescence, it becomes evident that slight cytoplasmic accumulation is present when cells are transfected with FLAG-hnRNP A1 F2 and that some nuclear retention is still present when cells are transfected with FLAG-hnRNP A1 ΔM9. Consequently, I believe this to be the central reason to the lack of a definable difference between the conditions and the

variability of Bcl-xL within the repeated experiments. In addition to this, it is possible that the lack of controlled nuclear accumulation when using the F2 mutant could be caused by the activation of a secondary, previously unidentified, region of hnRNP A1 that is also responsible for the localization mechanism. The same could also be said of an alternative post-translational modification which could regulate hnRNP A1's location and is not controlled for in this experiment. However, despite the lack of a clear overall trend in the expression of Bcl-xL, in regards to only the average of each condition, it could be plausible that a trend for Bcl-xL may present itself through further studies based on the slight increase observed while using the F2 mutant and, by comparison to this increase, the slight decrease when using the M9 mutant.

In response to stress, it is the regulation of IRES-mediated translation that has been shown to aid in the recovery of cells through the selective synthesis and inhibition of pro or anti-apoptotic proteins. However, it is when in the presence of extreme hypertonic shock that a cell will inhibit global protein synthesis, including the expression of proteins that serve to prevent apoptosis (Bevilacqua *et al*, 2010). As my results show that the expression of Bcl-xL, an anti-apoptotic protein which can be expressed using IRES-mediated translation, is altered in response to the presence of ARK5, the activation of caspases 3 and 7 were monitored to identify if through the knockdown and rescue of ARK5, could the viability of the cell be affected in kind. Remarkably, it is observed that the removal of ARK5 is shown to increase the viability of cells during stress (Figure 3.11 A). In contrast, change is minute when ARK5 is solely overexpressed to a concentration higher than the endogenous norm (Figure 3.11 B). Finally, although results show that the removal of ARK5 can increase the viability of cells by delaying the initial activation of caspase 3 and 7 by several hours compared to cells that are solely shocked, performing an ARK5

rescue results in a correlated increase in caspase activation. Consequently, this results in decreased viability and, to some degree, reverses the effects of ARK5's removal (Figure 3.11 B). Interestingly, to contradict these results, it has been noted in literature that during periods of stress brought on by nutrient starvation, ARK5 inhibits the expression of caspase 6 (Suzuki *et al,* 2004; Woods *et al,* 2005). This inhibition goes on to hinder the activation of caspase 8, which, when activated, allows for the activation of Bid, a pro-apoptotic member of the Bcl-2 family (Cowling and Downward, 2002). Once activated, Bid interacts with the mitochondrial membrane to release cytochrome c, eventually leading to the realization of the apoptotic signaling pathway (Li *et al,* 1998). Intriguingly, my results show that the removal of ARK5 is beneficial to U2OS cells undergoing hypertonic stress in terms that it delays the activation of caspases 3 and 7, therefore this identifies an alternative response to the identified link between ARK5 and caspase 6 in cells that undergo nutrient deprivation, which leads to the activation of apoptosis. Despite this difference, the regulation of caspase 6 was noted to be observed during nutrient deprivation and not hypertonic stress (Woods *et al,* 2005). As a cell's response to nutrient deprivation differs from that of hypertonic shock, I propose that despite the possibility of a contradiction in my results, the role of ARK5 to regulate the activation of caspase 6 differs when the cell is affected by hypertonic stress in lieu of nutrient deprivation. Overall, this data highlights that altering levels of ARK5, which modifies the subcellular location of hnRNP A1, affects the viability of the cell as a whole when under prolonged periods of stress, and I propose that this is in correlation with the previously identified alteration in Bcl-xL levels.

Conclusion

The regulation of protein synthesis is a highly regulated and complex mechanism used by cells to perform optimally and when faced with adverse conditions is a key adaptive mechanism capable of select protein synthesis to aid in its defense and eventual recovery. As such, my research serves to better understand and expand on the mechanisms surrounding stress response and the identification of a novel role for ARK5. Overall, these results provide evidence that ARK5 plays a key role in the localization of hnRNP A1 during hypertonic stress and that cells that lack ARK5 or whose activity is inhibited show concomitant reduction in hnRNP A1's cytoplasmic accumulation. In addition, evidence is shown that ARK5 directly interacts and phosphorylates hnRNP A1 somewhere within the C-terminal region, although the precise phosphorylation site(s) is yet to be determined. Finally, my research has provided confirmation that ARK5-dependent localization of hnRNP A1 regulates the expression of Bcl-xL and by extension shows altered viability during stress.

References

Allemand, E. *et al.* 2005. Regulation of heterogenous nuclear ribonucleoprotein A1 transport by phosphorylation in cells stressed by osmotic shock. *PNAS*. Vol. 102. p. 3602-3610

Baird, S. *et al.* 2006. Searching for IRES. *RNA.* Vol. 12. p. 1755-1785

Banerjee, S. *et al.* 2014. Characterization of WZ4003 and HTH-01-015 as selective inhibitors of the LKB1-tumour-suppresor-activated NUAK kinases. *Biochemical Journal*. Vol. 457. p. 215-225

Banerjee, S. *et al.* 2014. Interplay between Polo kinase, LKB1-activated NUAK1 kinase, $PP1\beta^{MYPT1}$ phosphatase complex and the $SCF^{\beta TrCP}$ E3 ubiquitin ligase. *Biochemical Society.* Vol. 461. p. 233-245

Barbosa, C. *et al*. 2013. Gene Expression Regulation by Upstream Open Reading Frames and Human Disease. *PLOS Genetics.* Vol. 9. p. 1-12

Bevilacqua, E. *et al*. 2010. eIF2α Phosphorylation Tips the Balance to Apoptosis during Osmotic Stress. *The Journal of Biological Chemistry*. Vol. 285. p. 17098-17111

Bonnal, S. *et al*. 2005. Heterogeneous Nuclear Ribonucleoprotein A1 Is a Novel Internal Ribosome Entry Site *trans*-Acting Factor That Modulates Alternative Initiation of Translation of the Fibroblast Growth Factor 2 mRNA. *The Journal of Biological Chemistry.* Vol. 280. p. 4144-4153

Brocker, C. *et al.* 2012. The role of hyperosmotic stress in inflammation and disease. *Biomol Concepts.* Vol. 3. p. 345-364

Burg, M. *et al.* 2007. Cellular Response to Hyperosmotic Stresses. *Physiol Rev*. Vol. 87. p. 1441-1474

Buxadé, M. *et al.* 2005. The Mnks Are Novel Components in the Control of TNFα Biosynthesis and Phosphorylate and Regulate hnRNP A1. *Immunity.* Vol. 23. p. 177-189

Cammas, A. *et al.* 2007. Cytoplasmic Relocalization of Heterogeneous Nuclear Ribonucleoprotein A1 Controls Translation initiation of Specific mRNAs. *Molecular Biology of the Cell.* Vol. 18. p. 5048-5059

Chang, X. *et al.* 2012. ARK5 is associated with the invasive and metastatic potential of human breast cancer cells. *J Cancer Research Clinical Oncology.* Vol. 138. p. 247-254

Chipuk, J. *et al.* 2006. Mitochondrial outer membrane permeabilization during apoptosis: the innocent bystander scenario. *Cell Death and Differentiation*. Vol. 13. p. 1396-1402

Coldwell, M. *et al.* 2000. Initiation of Apaf-1 translation by internal ribosome entry. *Oncogene.* Vol. 19. p. 899-905

Courteau, L. *et al.* 2015. Hexokinase 2 controls cellular stress response through localization of an RNA-binding protein. *Cell Death and Disease*. Vol. 6. p. 1-8

Cowling, V. and Downward, J. 2002. Caspase-6 is the direct activator of caspase-8 in the cytochrome c-induced apoptosis pathway: absolute requirement for the removal of caspase-6 prodomain. *Cell Death and Differentiation.* Vol. 9. p. 1046-1056

Damiano, F. *et al.* 2013. hnRNP A1 mediates the activation of the IRES-dependent SREBP-1a mRNA translation in response to endoplasmic reticulum stress. *Biochem J.* Vol. 449. p. 543-553

Durie, D. *et al.* 2011. RNA-binding protein HuR mediates cytoprotection through stimulation of XIAP translation. *Oncogene.* Vol. 30. p. 1460-1469

Fernandez, J. *et al. 2002.* Regulation of Internal Ribosome Entry Site-mediated Translation by Eukaryotic Initiation Factor-2α Phosphorylation and Translation of a Small Upstream Open Reading Frame. *The Journal of Biological Chemistry.* Vol. 277. p. 2050-2058

Fulda, S. *et al*. 2010. Cellular Stress Responses: Cell Survival and Cell Death. *International Journal of Cell Biology*. Vol. 2010. p. 1-23

Glisovic, T. *et al.* 2008. RNA-binding proteins and post-transcriptional gene regulation. *FEBS Letters*. Vol. 582. p. 1977-1986

Gradi, A. *et al.* 1998. Proteolysis of human eukaryotic translation initiation factor eIF4GII, but not eIF4GI, coincides with the shutoff of host protein synthesis after poliovirus infection. *Proc. Natl. Acad. Sci. USA.* Vol. 95. p. 11089-11094

Guil, S. *et al*. 2006. hnRNP A1 Relocalization to the Stress Granules Reflects a Role in the Stress Response. *Molecular and Cellular Biology*. Vol. 26. p. 5744-5758

Holcik, M. *et al.* 1999. A new internal-ribosome-entry-site motif potentiates XIAP-mediated cytoprotection. *Nature Cell Biology.* Vol. 1. p. 190-192

Holcik, M. *et al.* 2000. Internal ribosome initiation of translation and the control of cell death. *Translation and Cell Death*. Vol. 16. p. 469-473

Holcik, M. *et al.* 2003. The Internal Ribosome Entry Site-Mediated Translation of Antiapoptotic Protein XIAP Is Modulated by the Heterogeneous Nuclear Ribonucleoproteins C1 and C2. *Molecular and Cellular Biology.* Vol. 23. p. 280-288

Holcik, M. and Sonenberg, N. 2005. Translational Control in Stress and Apoptosis. *Molecular Cell Biology*. Vol. 6. p. 318-327

Holcik, M. 2015. Could the eIF2α-Independent Translation be the Achilles Heel of Cancer? *Frontiers in Oncology*. Vol. 5. p. 1-8

Hou, X. *et al.* 2011. A new role of NUAK1: directly phosphorylating p53 and regulating cell proliferation. *Oncogene.* Vol. 30. p. 2933-2942

Hu, Y. *et al.* 1998. Bcl-XL interacts with Apaf-1 and inhibits Apaf-1-dependent caspase-9 activation. *Proc. Natl. Acad. Sci. USA.* Vol. 95. p. 4386-4391

Iijima, M. *et al*. 2006. Two motifs for nuclear import of the hnRNP A1 nucleocytoplasmic shuttling sequence M9 core. *FEBS Letters*. Vol. 580. p. 1365-1370

Izaurralde, E. *et al.* 1997. A Role for the M9 Transport Signal of hnRNP A1 in mRNA Nuclear Export. *The Journal of Cell Biology*. Vol. 137. p. 27-35

Jean-Philippe, J. *et al.* 2013. hnRNP A1: The Swiss Army Knife of Gene Expression. *International Journal of Molecular Sciences.* Vol 14. p. 18999-19024

Jo, O. *et al.* 2008. Heterogeneous Nuclear Ribonucleoprotein A1 Regulates Cyclin D1 and c-*myc* Internal Ribosome Entry Site Function through Akt Signaling. *The Journal of Biological Chemistry.* Vol. 283. p. 23274-23287

Johannes, G. *et al.* 1999. Identification of eukaryotic mRNAs that are translated at reduced cap binding complex eIF4F concentrations using a cDNA microarray. *PNAS.* Vol. 96. p. 13118-13123

Kaboord, B. and Perr, M. 2008. Isolation of Proteins and Protein Complexes by Immunoprecipitation. *Methods in Molecular Biology.* Vol. 424. p. 349-364

Katz, M. *et al*. 2016. Hydroxylation and translational adaptation to stress: some answers lie beyond the STOP codon. *Cellular and Molecular Life Sciences*. Vol. 73. p. 1881-1893

Komar, A. and Hatzoglou, M. 2005. Internal Ribosome Entry Sites in Cellular mRNAs: Mystery of their existence. *The Journal of Biological Chemistry.* Vol. 280. p.23425-23428

Komar, A. and Hatzoglou, M. 2011. Cellular IRES-mediated translation the war of ITAFs in pathophysiological states. *Cell Cycle.* Vol. 10. p. 229-240

Komar, A. and Hatzoglou, M. 2015. Exploring internal ribosome entry sites as therapeutic targets. *Frontiers in Oncology*. Vol. 5. p. 1-10

Levin, M. *et al.* 2016. Autoantibodies to heterogeneous nuclear ribonuclear protein A1 (hnRNP A1) cause altered ribostasis and neurodegeneration; the legacy of HAM/TSP as a model of progressive sclerosis. *Journals in Neuroimmunology*. Vol. 304. p. 56-62

Lewis, S. *et al.* 2007. Subcellular Relocalization of *Trans*-acting Factor Regulates XIAP IRES-dependent Translation. *Molecular Biology of the Cell.* Vol. 18. p. 1302-1311

Lewis, S. and Holcik, M. 2007. For IRES *trans*-acting factors, it is all about location. *Oncogene*. p. 1-3

Li, G. *et al.* 2014. Quantifying absolute protein synthesis rates reveals principles underlying allocation of cellular resources. *Cell*. Vol. 157. p. 624-635

Li, H. *et al.* 1998. Cleavage of BID by Caspase 8 Mediates the Mitochondrial Damage in the Fas Pathway of Apoptosis. *Cell.* Vol. 94. p.491-501

Liwak, U. *et al*. 2012a. Translational Control in Apoptosis. *Experimental Oncology*. Vol. 34. p. 218-230

Liwak, U. *et al*. 2012b. Tumor Suppressor PDCD4 Represses Internal Ribosome Entry Site-Mediated Translation of Antiapoptotic Proteins and Is Regulated by S6 Kinase 2. *Molecular and Cellular Biology*. Vol. 32. p. 1818-1829

Lloyd, R. 2015. Nuclear Proteins Hijacked by Mammalian Cytoplasmic Plus Strand RNA Viruses. *Virology.* Vol. 0. p. 457-474

Lu, S. *et al.* 2013. ARK5 promotes glioma cell invasion, and its elevated expression is correlated with poor clinical outcome. *European Journal of Cancer.* Vol. 49. p. 752-763

Ma, X. *et al.* 2016. The NF-κB pathway participates in the response to sulfide stress in *Urechis unicintus*. *Fish and Shellfish Immunology.* Vol. 58. p. 229-238

Michael, W. *et al*. 1995. Signal Sequences That Target Nuclear Import and Nuclear Export of Pre-mRNA-binding Proteins. *Cold Spring Harbor Symposia on Quantitative Biology*. Vol. 60. p. 663-668

Nakielny, S. *et al*. 1996. Transportin: Nuclear Transport Receptor of a Novel Nuclear Protein Import Pathway. *Experimental Cell Research.* Vol. 229. p. 261-266

Perrotti, D. and Neviani, P. 2007. From mRNA Metabolism to Cancer Therapy: Chronic Myelogenous Leukemia Shows the Way. *Clinical Cancer Research.* Vol. 13. p. 1638-1642

Piñol-Roma, S. *et al.* 1988. Immunopurification of heterogeneous nuclear ribonucleoprotein particles reveals an assortment of RNA-binding proteins. *Genes & Development*. Vol. 2. p. 215-227

Ray, P. *et al.* 2006. Two internal ribosome entry sites mediate the translation of p53 isoforms. *EMBO Reports.* Vol. 7. p. 404-410

Rebane, A. *et al.* 2004. Transportins 1 and 2 are redundant nuclear import factors for hnRNP A1 and HuR. *RNA*. Vol. 10. p. 590-599

Reményi, A. *et al.* 2006. Docking interaction in protein kinase and phosphatase networks. *Current Opinion in Structural Biology.* Vol. 16. p. 676-685

Richard, J. *et al.* 2010. The mechanism of eukaryotic translation initiation and principles of its regulation. *Molecular Cell Biology.* Vol. 10. p. 133-127

Roy, R. *et al.* 2014. hnRNP A1 couples nuclear export and translation of specific mRNAs downstream of FGF-2/S6K2 signaling. *Nucleic Acids Research.* Vol. 42. p. 12482-12497

Samali, A. *et al.* 1999. Thermotolerance and cell death are distinct cellular responses to stress: dependence on heat shock proteins. *FEBS*. Vol. 461. p. 306-310

Sigoillot, F. and King, R. 2011. Vigilance and Validation: Keys to Success in RNAi Screening. *ACS Chem Biol*. Vol. 6. p. 47-60

Siomi, H. and Dreyfuss, G. 1995. A Nuclear Localization Domain in the hnRNP A1 Protein. *The Journal of Cell Biology.* Vol. 129. p. 551-560

Spriggs, K. *et al*. 2005. Internal ribosome entry segment-mediated translation during apoptosis: the role of IRES-*trans*-acting factors. *Cell Death and Differentiation*. Vol. 12. p. 585-591

Stonely, M. *et al.* 1998. C-Myc 5' untranslated region contains an internal ribosome entry segment. *Oncogene.* Vol. 16. p. 423-428

Sun, X. *et al.* 2013. The regulation and function of the NUAK family. *Journal of Molecular Endocrinology.* Vol. 52. p. 15-22

Suzuki, A. *et al.* 2003. Identification of Novel Protein Kinase Mediating Akt Survival Signaling to the ATM Protein. *The Journal of Biological Chemistry.* Vol. 278. p. 48-53

Suzuki, A. *et al.* 2004. Regulation of caspase-6 and FLIP by the AMPK family member ARK5. *Oncogene.* Vol. 23. p. 7067-7075

Sweeney, T. *et al.* 2012. A Distinct Class of Internal Ribosomal Entry Site in Members of the *Kobuvirus* and Proposed *Salivirus* and *Paraturdivirus* Genera of the *Picornaviridae. Journal of Virology.* Vol. 86. p. 1468-1486

Twyffles, L. *et al.* 2014. Transportin-1 and Transportin-2: Protein nuclear import and beyond. *Federation of European Biochemical Societies.* Vol. 588. p. 1857-1868

Um, H. 2015. Bcl-2 family proteins as regulators of cancer cell invasion and metastasis: a review focusing on mitochondrial respiration and reactive oxygen species. *Oncotarget.* Vol. 7. p. 5193-5203

Van der Houven van Oordt, W. *et al.* 2000. The $MKK_{3/6}$-p38-signaling Cascade Alters the Subcellular Distribution of hnRNP A1 and Modulates Alternative Splicing Regulation. *The Journal of Cell Biology.* Vol. 149. p. 307-316

Wang, X. *et al.* 2004. Bcl-xL disrupts death-inducing signal complex formation in plasma membrane induced by hypoxia/reoxygenation. *The FASEB Journal.* Vol. 18. p. 1826-1833

Woods, A. *et al. 2005.* Ca^{2+}/calmodulin-dependent protein kinase kinase-β acts upstream of AMP-activated protein kinase in mammalian cells. *Cell Metabolism.* Vol. 2. p. 21-33

Appendix

siRNA Target Sequences (5' - 3'):

- siControl: AAUUCUCCGAACGUGUCACGU
- siARK5 #1: AGGAGUGCUGUGAUUGACUAGUAAU
- siARK5 #2: CGGCAGGACUCUUAUCUUA

Primer Sequences (5' - 3') (Mutations are underlined):

- hnRNP A1 SASSS Mutant 1 Forward:
  AGAGATGGCTGCTGCTGCAGCCAGCCAAAGAGGTCG

- hnRNP A1 SASSS Mutant 1 Reverse:
  CGACCTCTTTGGCTGGCTGCAGCAGCAGCCATCTCT

- hnRNP A1 SASSS Mutant 2 Forward:
  AGCAAGAGATGGCTGCTGCTGCAGCCGCCCAAAGAGGTCG

- hnRNP A1 SASSS Mutant 2 Reverse:
  CGACCTCTTTCGGCGGCTGCAGCAGCAGCCATCTCTTGCT

- hnRNP A1 Fragment 1 (nuc. 1-258) Forward:
  CCGGAATTCATGGATTACAAGGACGACGACGATAAGTCTAAGTCAGAGTCTC
  CTAAAGAG

- hnRNP A1 Fragment 1 (nuc. 1-258) Reverse:
  ACTGTCTAGATTATGGTTCCACAACTCTTCC

- hnRNP A1 Fragment 2 (nuc. 259-633) Forward:
  ACTGGAATTCATGGACTACAAAGACGATGACGACAAGAAGAGAGCTGTCTCC
  AGAG

- hnRNP A1 Fragment 2 (nuc. 259-633) Reverse:
  ACTGTCTAGATTAACCGAAACCACCTCCACG

- hnRNP A1 Fragment 3 (nuc. 634-963) Forward:
  ACTGGAATTCATGGACTACAAAGACGATGACGACAAGGGGAATGACAACTTC
  GGTG

- hnRNP A1 Fragment 3 (nuc. 634 – 963) Reverse:
  TGCTCTAGATTAAAATCTTCTGCCACTGCC

Plasmid Information:

Table 1: Plasmids used and their vectors

Name of Plasmid:	**Plasmid Vector:**
Kate (EV)	pmKate2-C
FLAG	pcDNA3
GST	pGEX4T-1
SAMS	pGEX4T-1
ARK5-GST	pDEST27
His-hnRNP A1	pTrcHis
FLAG-hnRNP A1	pCI
FLAG-hnRNP A1 ΔM9	pcDNA3
FLAG-hnRNP A1 F2	pcDNA3
FLAG-hnRNP A1 SASSS Mutant 1	pcDNA3
FLAG-hnRNP A1 SASSS Mutant 2	pcDNA3
FLAG-hnRNP A1 Fragment 1 (nucleotides 1-258)	pcDNA3
FLAG-hnRNP A1 Fragment 2 (nucleotides 259-633)	pcDNA3
FLAG-hnRNP A1 Fragment 3 (nucleotides 634-963)	pcDNA3
FLAG-hnRNP A1 Fragment 1+2 (nucleotides 1-633)	pcDNA3
FLAG-hnRNP A1 Fragment 2+3 (nucleotides 259-963)	pcDNA3

Antibody Conditions:

Table 2: Immunoblotting conditions

Antibody Name	**Block Incubation** (1 hour at room temperature)	**Primary AB Incubation** (Overnight at 4°C)	**Secondary AB Incubation** (1 hour at room temperature)
ARK5 (Cell Signal Cat.# 4458) (Source: Rabbit)	5% Skim Milk in TBS-T	1:1000 dilution in 2.5% BSA in TBS-T	1:1000 Anti-Rabbit dilution in 2.5% BSA in TBS-T
Bcl-xL (Cell Signal Cat.# 2762) (Source: Rabbit)	5% BSA in PBS-T	1:1000 dilution in 5% BSA in PBS-T	1:2000 Anti-Rabbit dilution in 5% BSA in PBS-T
hnRNP A1 (Sigma Cat.# R9778) (Source: Mouse)	5% Skim Milk in TBS-T	1:10000 dilution in 5% Skim Milk in TBS-T	1:10000 Anti-Mouse dilution in 5% Skim Milk in TBS-T
Alpha Tubulin (Abcam Cat.# ab7291) (Source: Mouse)	5% BSA in PBS-T	1:10000 dilution in PBS-T (O/N or 1 hour)	1:10000 Anti-Mouse dilution in PBS-T
FLAG (DYKDDDDK Tag) (Cell Signal Cat.# 8146) (Source: Mouse)	5% Skim Milk in TBS-T	1:1000 dilution in 5% BSA in TBS-T	1:1000 Anti-Mouse dilution in 5% BSA TBS-T

Secondary antibody information:

- Anti-Rabbit: Anti-rabbit IgG, HRP-linked (Cell Signal Cat.# 7074)
- Anti-Mouse: Anti-mouse IgG, HRP-linked (Cell Signal Cat.# 7076)

Table 3: Immunofluorescence conditions

Antibody Name	**Primary AB Incubation** (1 hour at room temperature)	**Secondary AB Incubation** (1 hour at room temperature)
hnRNP A1 (Sigma Cat.# R9778) (Source: Mouse)	1:300 dilution in Triton X-100/BSA buffer solution	1:1000 Anti-Mouse dilution in Triton X-100/BSA buffer solution
FLAG (DYKDDDDK Tag) (Cell Signal Cat.# 8146) (Source: Mouse)	1:1000 dilution in Triton X-100/BSA buffer solution	1:1000 Anti-Mouse dilution in Triton X-100/BSA buffer solution

Secondary antibody information:

- Anti-Mouse: Alexa Fluor® 488 goat anti-mouse IgG (H+L) (Thermo Fisher Cat.# A11001)

Curriculum Vitae

TRAVIS RICHARD

OBJECTIVE

To explore career opportunities in biochemistry and molecular biology. My long-term goal is to further expand on my knowledge of biochemistry and related lab based techniques, leading to a career in the health sciences industry.

EDUCATION

Master's Degree, Biochemistry — September 2014 to Present
University of Ottawa

Bachelor of Science, Biochemistry - Honours — May 2014
Université de Moncton

Diploma of Health Sciences — May 2012
Université de Moncton

Groupe Pont Immersion Program — May 2011
Université de Moncton

SKILLS & ABILITIES

Research / Laboratory Techniques:

- Biochemistry and Molecular Biology: DNA and RNA extraction, Plasmid DNA preparation, Plasmid transformation, Restriction enzyme digests, PCR, Quantitative PCR, Reverse transcription PCR, Agarose gel electrophoresis, SDS-PAGE electrophoresis, Cell fractionation by centrifugation, Primer sequence design, Spectroscopy (UV and Visible), Sequence alignment/analysis, Western blotting, Chloroform and phenol extraction, Cell culture techniques, siRNA mediated knockdown, Viral infection, Bradford assay, Cell lysis, Ponceau S and Coomassie blue staining, *In vitro* kinase assay, Radioactivity management, Column chromatography and bead based protein purification, Cloning, Site-directed mutagenesis, Immunofluorescent staining, Drug administration, Cell viability and cytotoxicity analysis
- Microbiology: Aseptic and sterile techniques, Optical microscopy, Fluorescent microscopy, Confocal microscopy, Bacterial staining, Plating methods, Immunofluorescence, Bacterial cell culture
- Chemistry: Solution preparation, Titrations, Extraction filtration, Simple and fractional distillation, Solubility tests, Determination of index refraction, Recrystallization
- Computer: Extensive use of Word, Excel, PowerPoint and Photoshop, Working knowledge of analytical biochemical programs (IncuCyte Zoom Image Analyser, Image Studio, Prism, Columbus Image Analyser, Biogazelle Qbase+, DNAMAN, REST 2009)

Professional:

- Communication skills strengthened as a coach for a master's swim team, lifeguarding team captain, office management and park supervisory for water amusement park
- Teamwork skills gained through laboratory work and courses, and employment in the recreation and leisure industry (lifeguarding)
- Exceptional organizational and time management skills

Leadership:

- Office Management / Operations Supervisor for water amusement park
- Lifeguard team captain
- Swimming coach and instructor
- Student recruitment ambassador for Université de Moncton

Languages:

- English - Native language
- French - Proficient in speaking, reading and writing

Certifications:

WHIMIS and Occupational Health and Safety

Canadian Red Cross First Responder CPR Level C & AED

Exceptional Service Seminar – Customer Service Training

EXPERIENCE

University of Ottawa – Dr. Martin Holcik's Lab, Ottawa, ON — September 2014 to Present
Researcher

Master's Degree Research position responsible for the analysis of ARK5's role in the stress response of cancer cells in regards to the localization of hnRNP A1

Université de Sherbrooke – 2016 RiboClub Annual Conference — September 2016
Presenter

Presentation of Master's Research in the form of a poster

University of Ottawa – BMI Graduate Research Seminar Day — March 2016
Presenter

Presentation of Master's Research in the form of a seminar

First place prize in MSc Biochemistry category

University of Ottawa – BMI Graduate Research Poster Day — May 2015
Presenter

Presentation of Master's Research in the form of a poster

Université de Moncton – Labo de Dr. Pier Jr Morin, Moncton, NB — September 2014
Published paper – Second Author

Review - Mammalian Hibernation and Regulation of Lipid Metabolism: A Focus on Non-coding RNAs - Biochemistry (Moscow), 2014, Vol. 79, No 11. pp. 1161-1171.

Université de Moncton – Labo de Dr. Pier Jr Morin, Moncton, NB — May 2013 to May 2014
Researcher

Honours Research position responsible for the analysis of amplification and expression of microRNA's in a hibernating mammal

Université de Moncton – 25e Colloque des jeunes chercheuses et chercheurs — March 2014
Presenter

Presentation of Honours Research in the form of a poster

AWARDS AND SCHOLARSHIPS

- BMI Graduate Research Seminar Day – MSc Biochemistry Category – First Place — March 2016
  University of Ottawa
- Certificat de Mérite – Excellents Résultats Académiques 2013-2014 — October 2014
  Université de Moncton
- Bourse de Recherche d'Été — May 2013
  Université de Moncton
- Bourse d'Accueil de Mérite Académique — June 2009
  Université de Moncton
- Bourse Patrimoine Canadien – Minorités — June 2009
  Université de Moncton
- Advanced French Oral Proficiency Certification — June 2009
  Moncton High
- John MacPherson Memorial Bursary — June 2009
  Moncton High
- Lou MacNarin Home & School Bursary — June 2009
  Moncton High